EUCALL Joint Foresight Topical Workshop on Theory and Simulation of Photon-Matter Interaction, Szeged, July 1-5, 2018

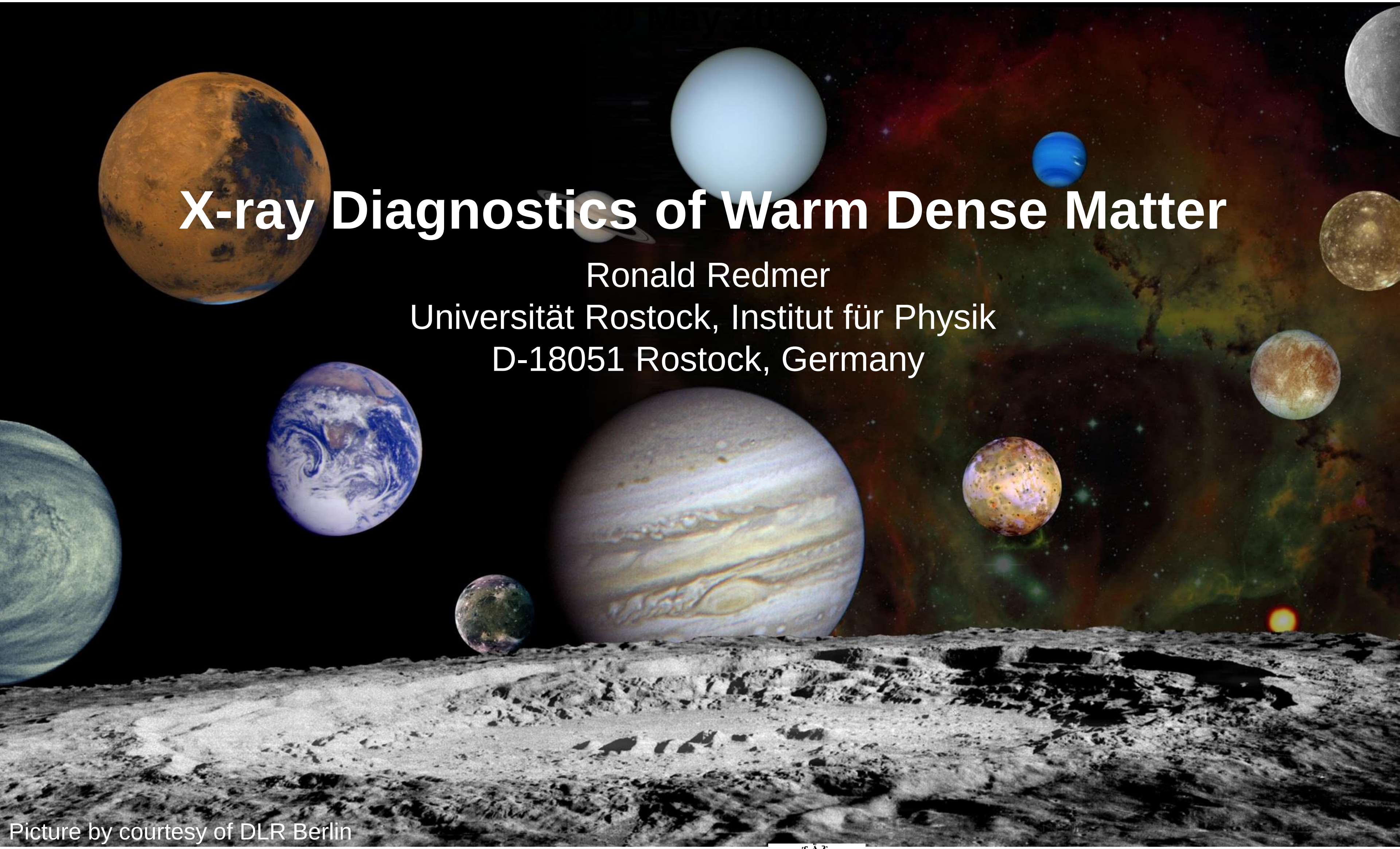

X-ray Diagnostics of Warm Dense Matter

Ronald Redmer
Universität Rostock, Institut für Physik
D-18051 Rostock, Germany

Picture by courtesy of DLR Berlin

Bundesministerium für Bildung und Forschung

DFG Deutsche Forschungsgemeinschaft

INSTITUT FÜR PHYSIK

SFB 652

Acknowledgements

SFB 652
BMBF FSP 301
BMBF FSP 302
DFG SPP 1385
DFG SPP 1488
DFG SPP 1992
FOR 2440
HLRN

Andreas Becker
Mandy Bethkenhagen
Thomas Bornath
Richard Bredow
Daniel Cebulla
Martin French
Clemens Kellermann
Nadine Nettelmann
Anna-Julia Poser
Kai-Uwe Plagemann
Martin Preising
Ludwig Scheibe
Manuel Schöttler
Philipp Sperling
Bastian Witte

Contents

Astrophysical objects

Extreme states of matter

Giant Planets $M<13M_J$	Brown Dwarfs $13M_J<M<75M_J$	Stars $M>75M_J$

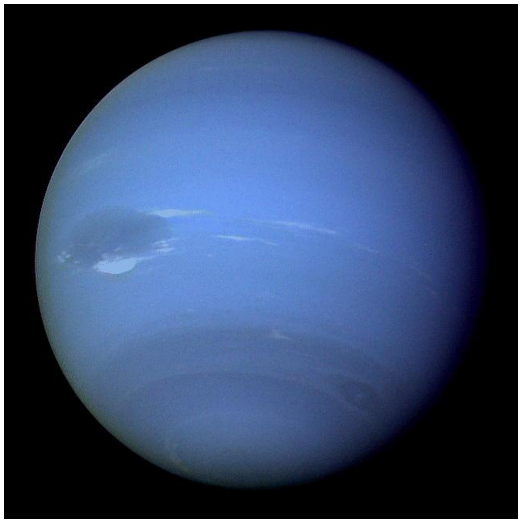

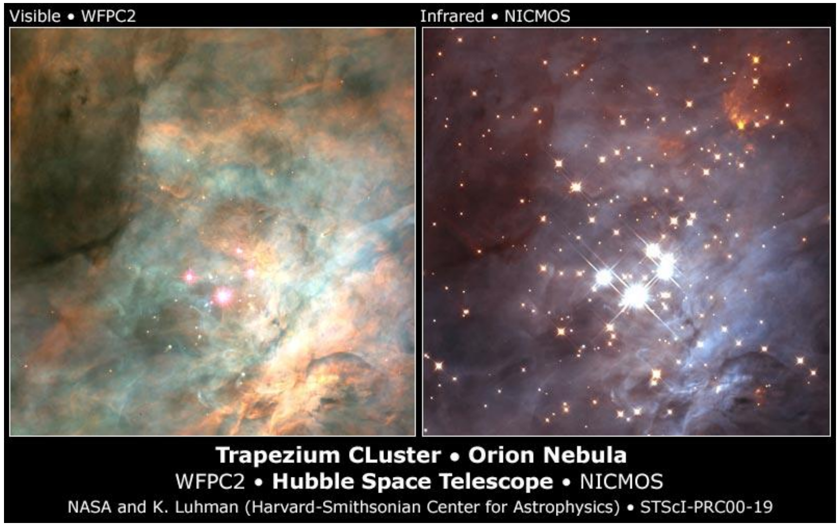

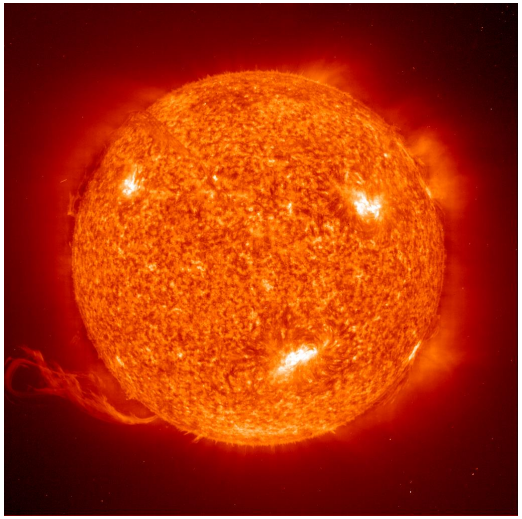

J, S, U, N and many extrasolar planets	… in the Orion Nebula seen in the IR spectrum	The Sun
Core (e.g. Jupiter): $\approx 2\text{x}10^4$ K & 40 Mbar **warm dense matter**	Cores (e.g. Gliese 229B): $\approx 10^6$ K & 100 Gbar **degenerate matter**	Core of the Sun: $\approx 15\text{x}10^6$ K & 250 Gbar **hot dense matter**

Warm Dense Matter (WDM)

See: Basic Research Needs for High Energy Density Laboratory Physics (DOE Office of Science and NNSA, 2010)

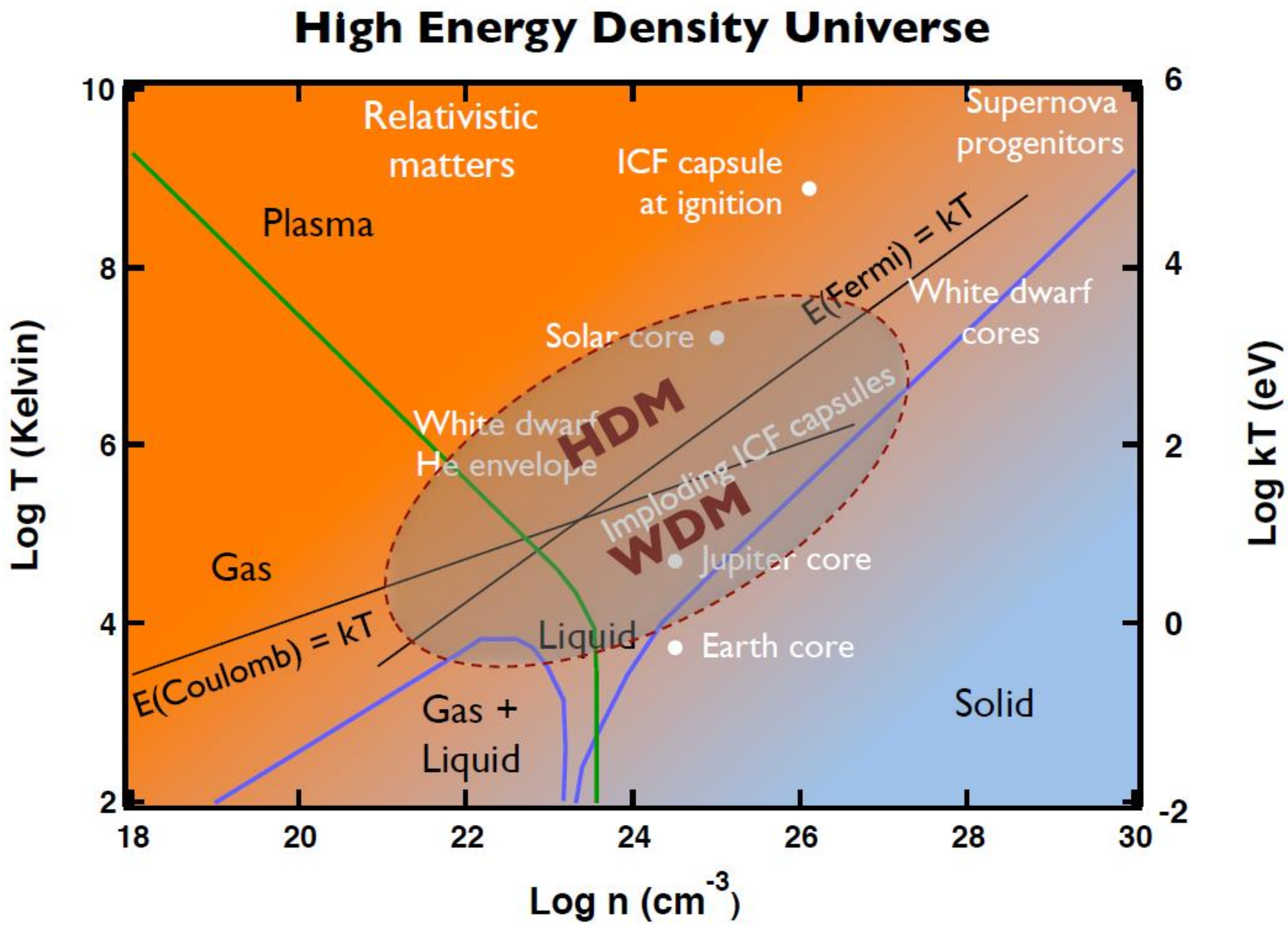

DENSITY ~ solid density (0,1 – 10)
TEMPERATURE ~ few eV
PRESSURES ~ Mbar-Gbar

Warm Dense Matter (WDM)

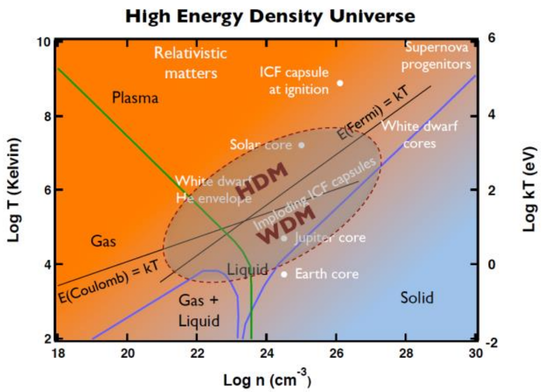

Inertial Confinement Fusion (courtesy NIF)

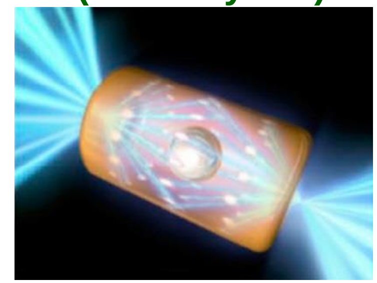

$T > 10^8$ K
P > 100 Gbar

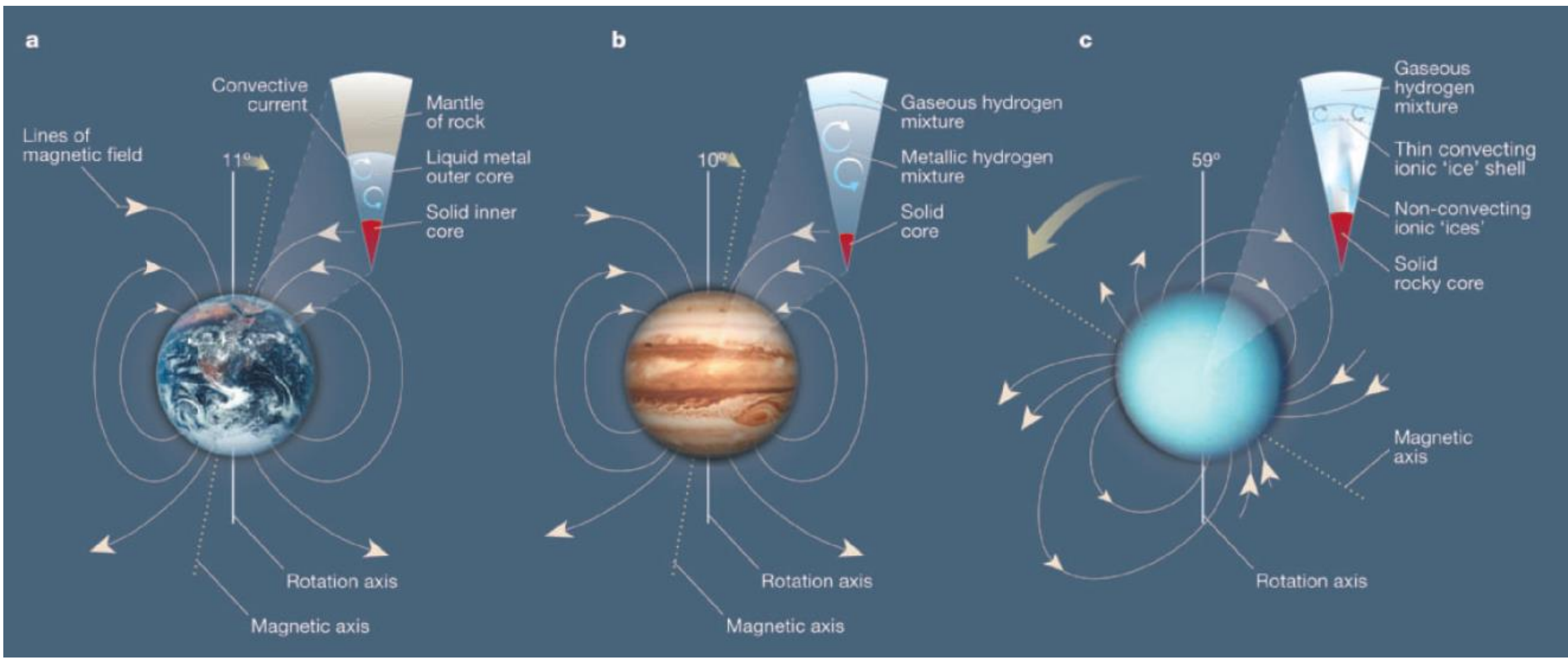

Interior and magnetic field of Solar Sytem planets, see J. Aurnou, Nature 428, 134 (2004)

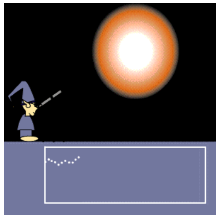

Extrasolar transiting planets

Mean density vs. mass

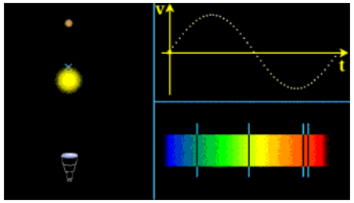

H. Rauer et al., Exp. Astron. **38**, 249 (2014)

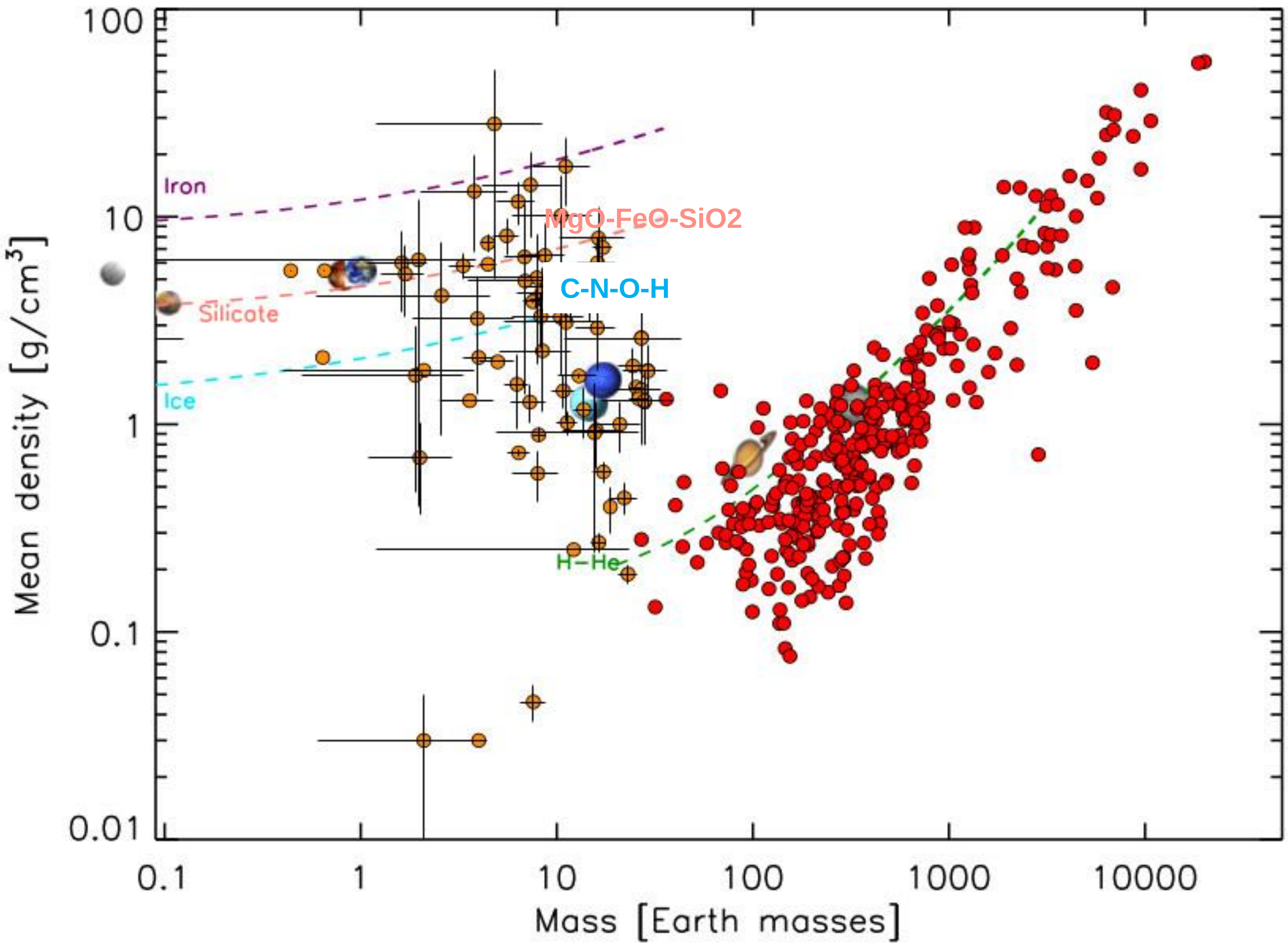

Basic equations for planetary modeling

mass conservation:

$$dm = 4\pi r^2 \rho(r)\, dr$$

hydrostatic equation of motion:

$$\frac{1}{\rho}\frac{dP}{dr} = \frac{dU}{dr}\ , \qquad U = V + Q$$

gravitational potential:

$$V(\vec{r}) = -G\int_{V_0} d^3r'\,\frac{\rho(r')}{\left|\vec{r}-\vec{r}\,'\right|}$$

expansion into Legendre polynomials:

$$V(r,\theta) = -\frac{GM}{r(\theta)}\left(1-\sum_{i=1}^{\infty}\left(\frac{R_{eq}}{r(\theta)}\right)^{2i} J_{2i}P_{2i}\left(\cos\theta\right)\right)$$

gravitational moments:

$$J_{2i} = -\frac{1}{MR_{eq}^{2i}}\int d^3r'\,\boxed{\rho(r'(\theta'))}\,r'^{2i}\,P_{2i}(\cos\theta')$$

Calculations via theory of figures (Zharkov & Trubitsyn)
with boundary conditions $M_p(R_p)$, Y_1, $\bar{Y}$, P and T at 1 bar.
Mass distribution along (piecewise) isentropes/isotherms according to EOS data for WDM – most important input!

Interior of Gas Giants: H-He

Three-layer model, input and constraints

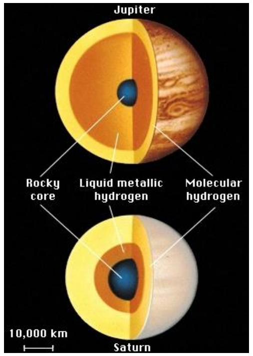

Atmosphere models (luminosity, abundances)

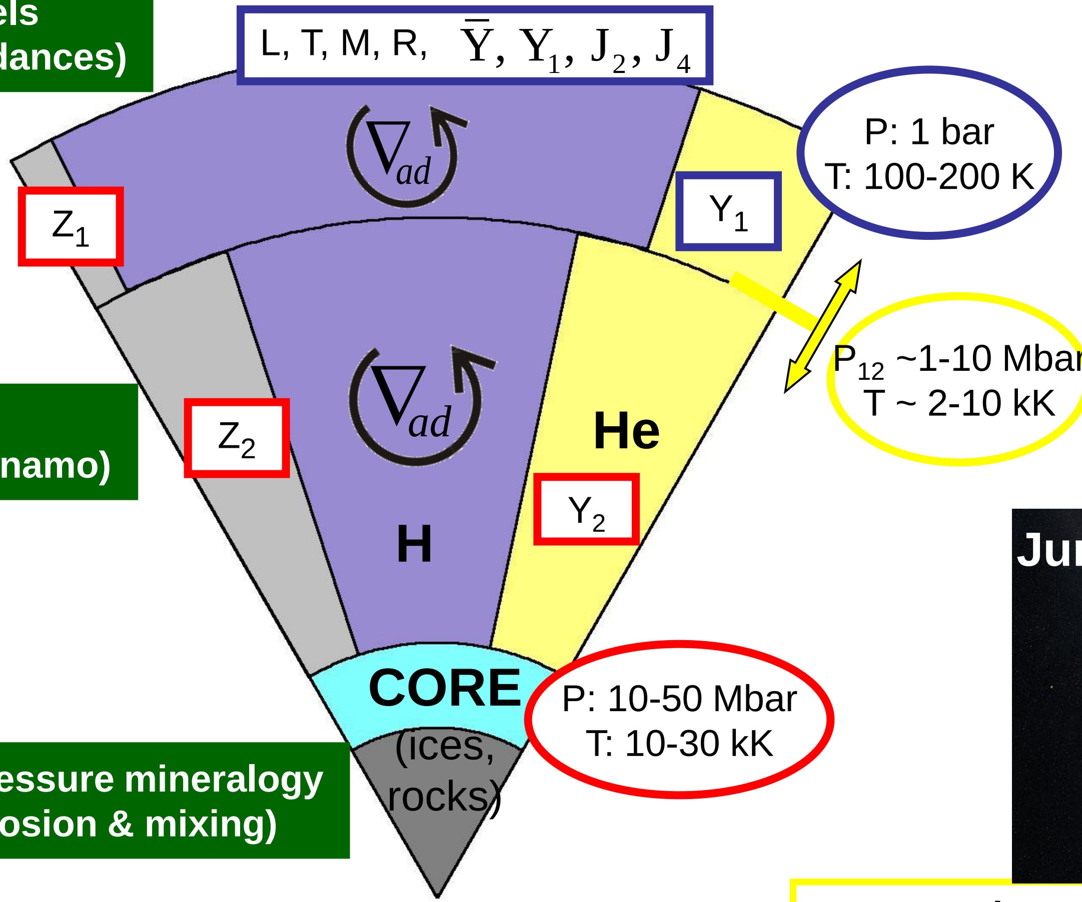

Magnetic field generation (dynamo)

High-pressure mineralogy (core erosion & mixing)

- constraints (blue)
- results from modeling (red)
- free parameter (yellow)

Physical origin and location of the layer boundary:
→ MIT (PPT)
→ H-He demixing

Matter under extreme conditions (WDM):
- High-pressure H-He phase diagram
- EOS of complex mixtures
- Electrical & thermal conductivity
- Diffusion & viscosity

See e.g. D.J. Stevenson (1982), T. Guillot (1999), N. Nettelmann et al. (2008, 2012)

High-pressure phase diagram of H

Jupiter, Saturn, hot Jupiters
Metalization & Plasma Phase Transition
H-He demixing

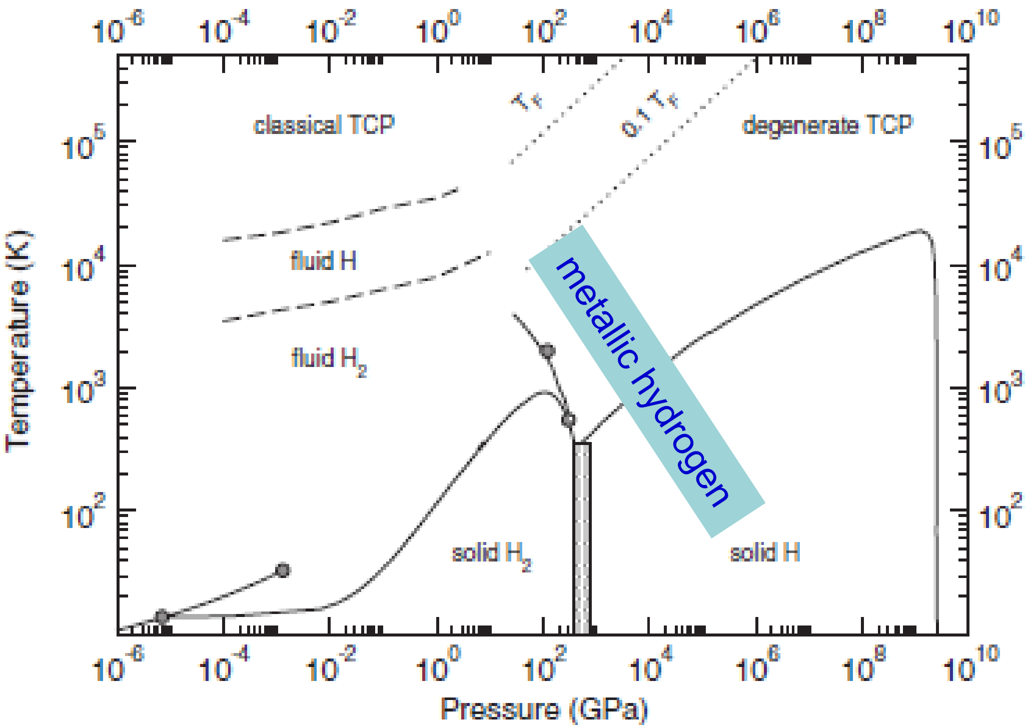

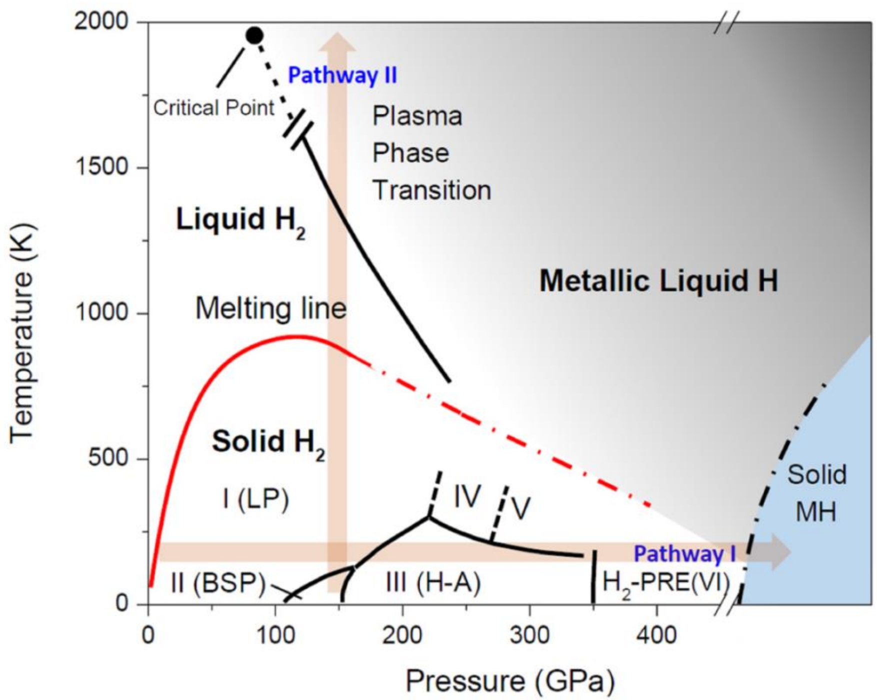

J.M. McMahon et al., RMP **84**, 1607 (2012)

R.P. Dias, I.F. Silvera, Science (2017)
For recent DAC studies, see also:
P. Dalladay-Simpson et al., Nature (2016)
R.S. McWilliams et al., PRL (2016)

Interior of Ice Giants: C-N-O-H mixtures

Multi-layer models

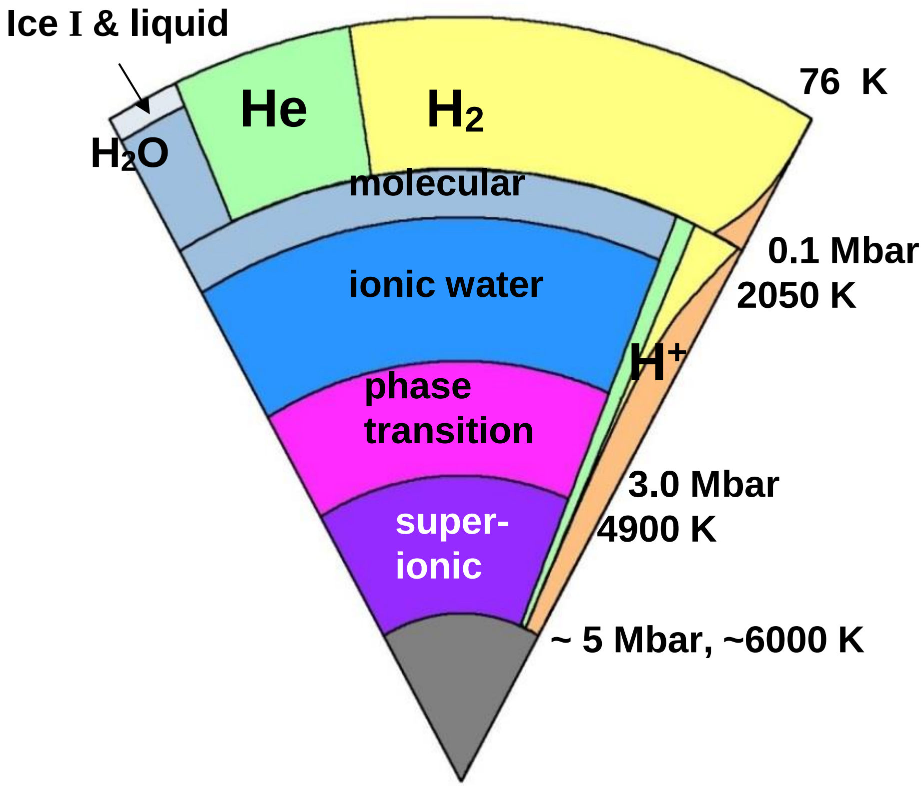

U & N
Neptune-like exos
mini-Neptunes

Physical origin and location of layer boundaries:
→ ice phase diagram
→ superionic phase?
→ carbon rain?
→ solubility of rock material?
→ inhomogeneous zone from formation: thermal boundary layer?

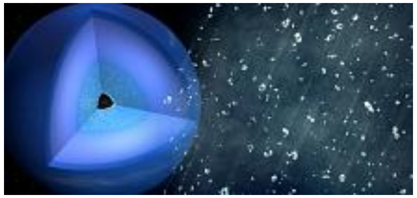

D. Kraus et al., Nat. Astron. **1**, 606 **(**2017)

Interior structure models of this type are not uniquely defined.
Accurate EOS data for warm dense C-N-O-H-He mixtures are needed and information on the high-P phase diagram.

See e.g. Hubbard et al. (1980, 89, 95), Helled et al. (2009, 10, 11), Nettelmann et al. (2013)

High-pressure phase diagram of H_2O

H_2O: see RR et al., Icarus **211**, 798 (2011)
NH_3: M. Bethkenhagen, M. French, RR, JCP **138**, 234504 (2013)
NH_3-H_2O: M. Bethkenhagen et al. JPCA **119**, 10582 (2015)
C-N-O-H: M. Bethkenhagen et al. ApJ **848**, 67 (2017)

Uranus (white), Neptune (black), ice giants, mini-Neptunes

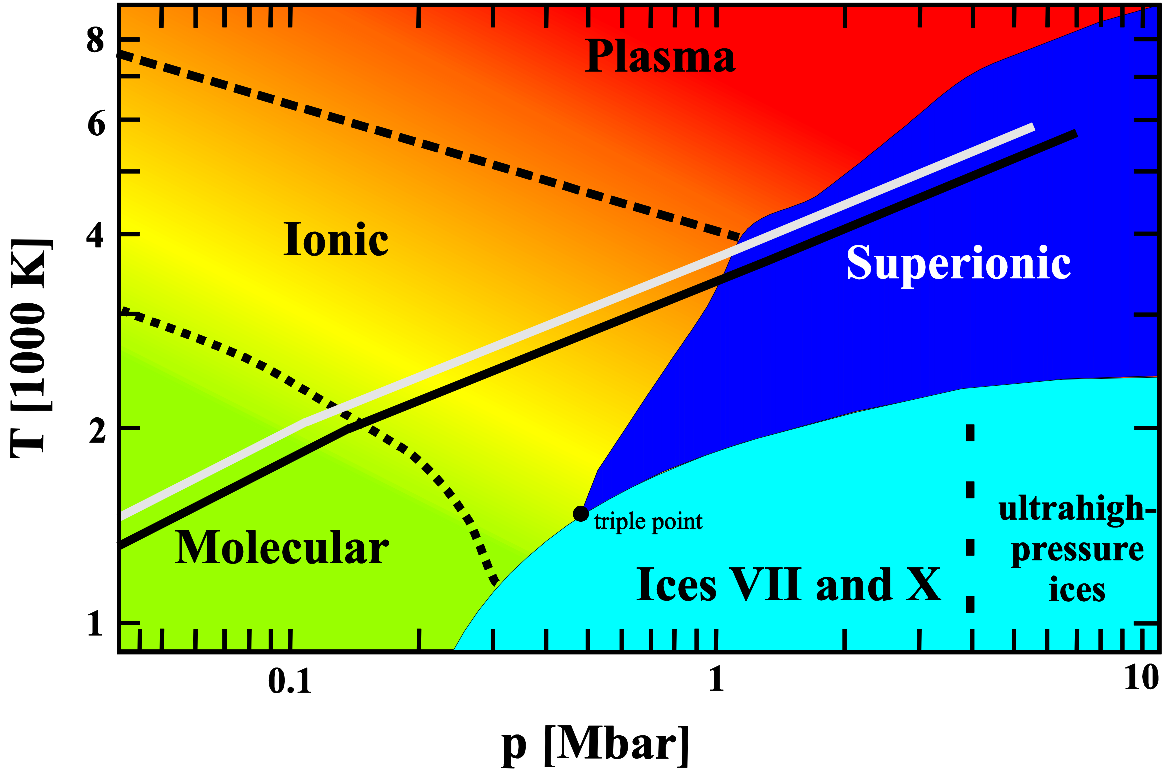

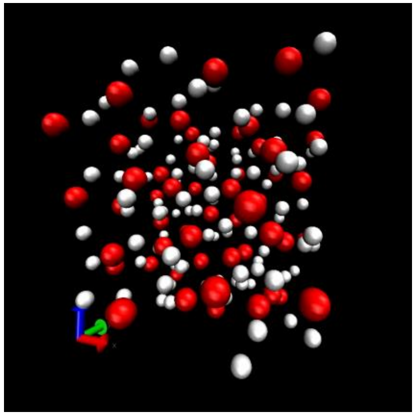

C. Cavazzoni et al.,
Science **283**, 44 (1999)
T.R. Mattsson, M.P. Desjarlais,
PRL **97**, 017801 (2006)
E. Schwegler et al.,
PNAS **105**, 14779 (2008)
H.F. Wilson et al.,
PRL **110**, 151102 (2013)

EOS and phase diagram:
M. French et al., PRB **79**, 054107 (2009), PRE **93**, 022140 (2016)
Transport properties (diffusion, conductivity):
M. French et al., PRB **82**, 174108 (2010), PoP **24**, 092306 (2017)

Contents

Diamond Anvil Cells (DACs)

By courtesy of H.-P. Liermann (DESY)

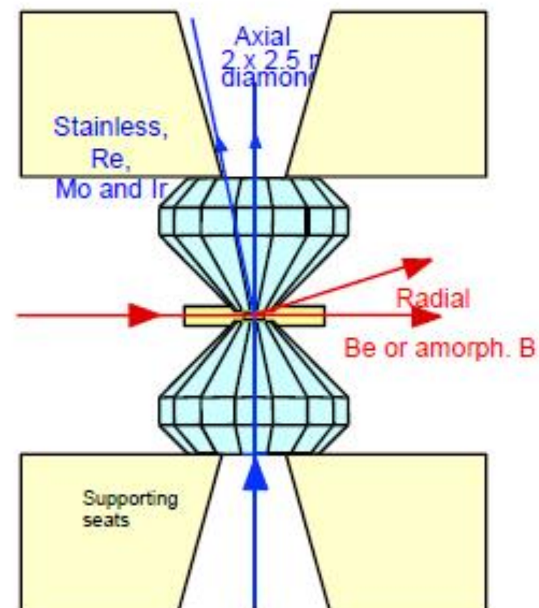

Conventional DAC technique is limited to static pressures of few Mbar and low T using resistive or pulsed laser heating.

Dynamic dDAC (for molecular solids) > 2 Mbar
Evans et al. 2007
Double-stage dsDAC – potential to reach 10 Mbar
Dubrovinsky et al. 2012: Re >6 Mbar
Dubrovinsky et al. 2015: Os ~8 Mbar
X-ray diagnostics at 3rd generation synchrotrons:
- ESRF, ECB@PETRA III, APS, Diamond …
- Structure, phase transitions, EOS, reflectivity …

Laser-driven shocks: NIF, Omega, Nike … Orion, Vulcan, LMJ, LULI, PeTAL, Phelix …

Combination of pre-compressed samples (DACs) and shock waves (lasers)
Jeanloz et al. 2007, Eggert et al. 2008,
Loubeyre et al. 2012, Torchio et al. 2016

Shock waves: Hugoniot curve for H_2O

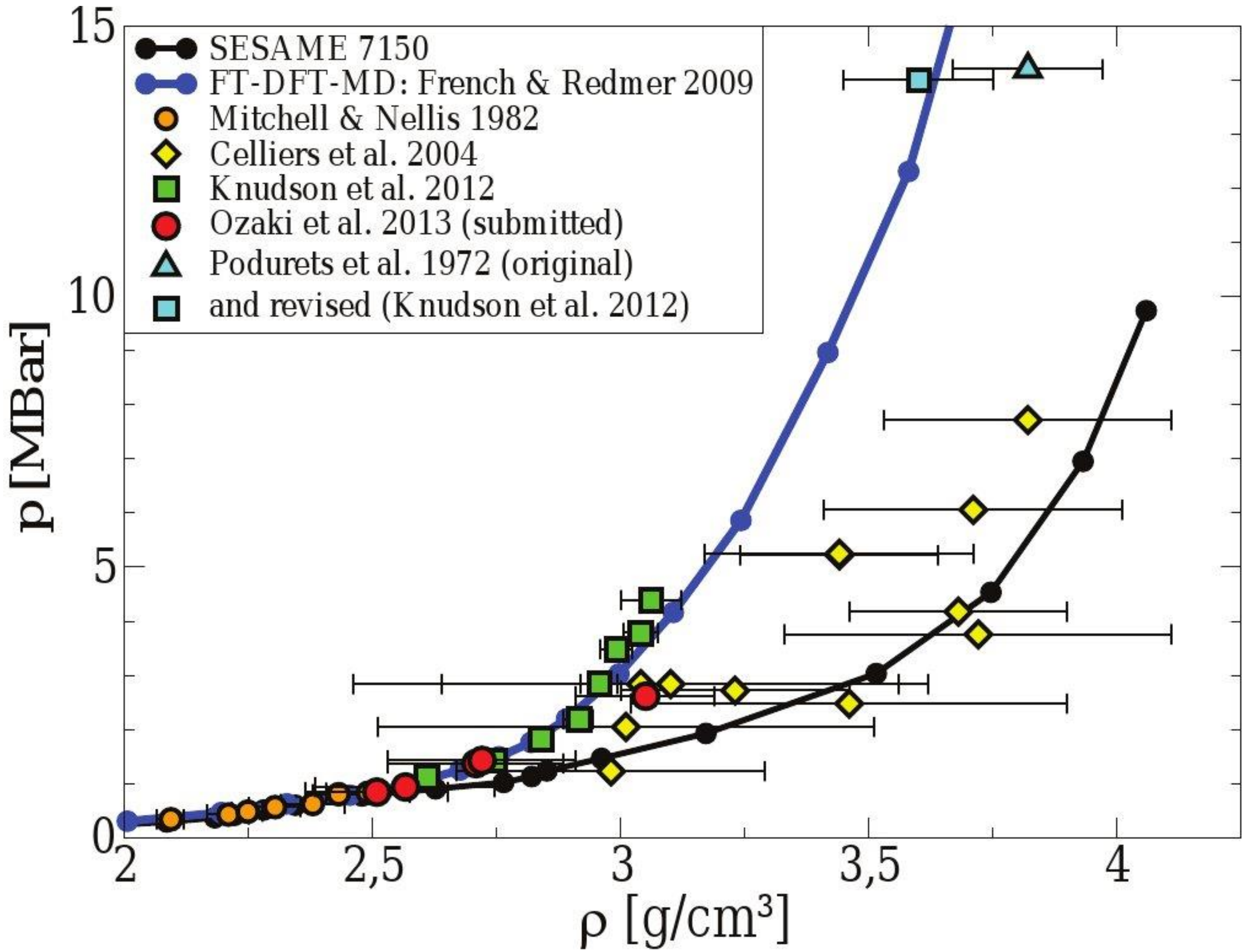

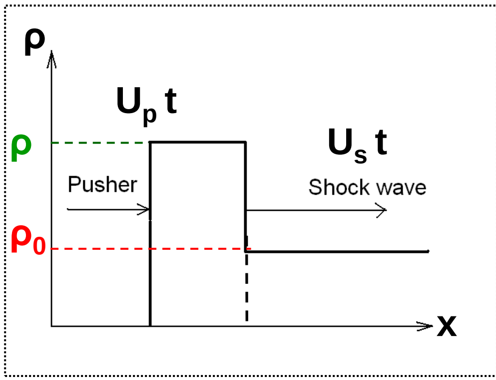

Data:
Red ◊ □ : Sandia Z
Open □ : Laser shocks
Theory: FT-DFT-MD
Red: HSE
Magenta: PBE

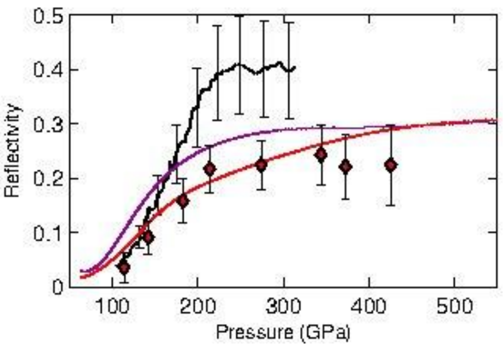

M.D. Knudson et al., PRL 1**08**, 091102 (2012) – Sandia Z machine

X-ray scattering:

$$\lambda_{crit} = \frac{2\pi c}{\omega_{pl}} \qquad \omega_{pl} = \sqrt{\frac{e^2 n_e}{\epsilon_0 m_e}}$$

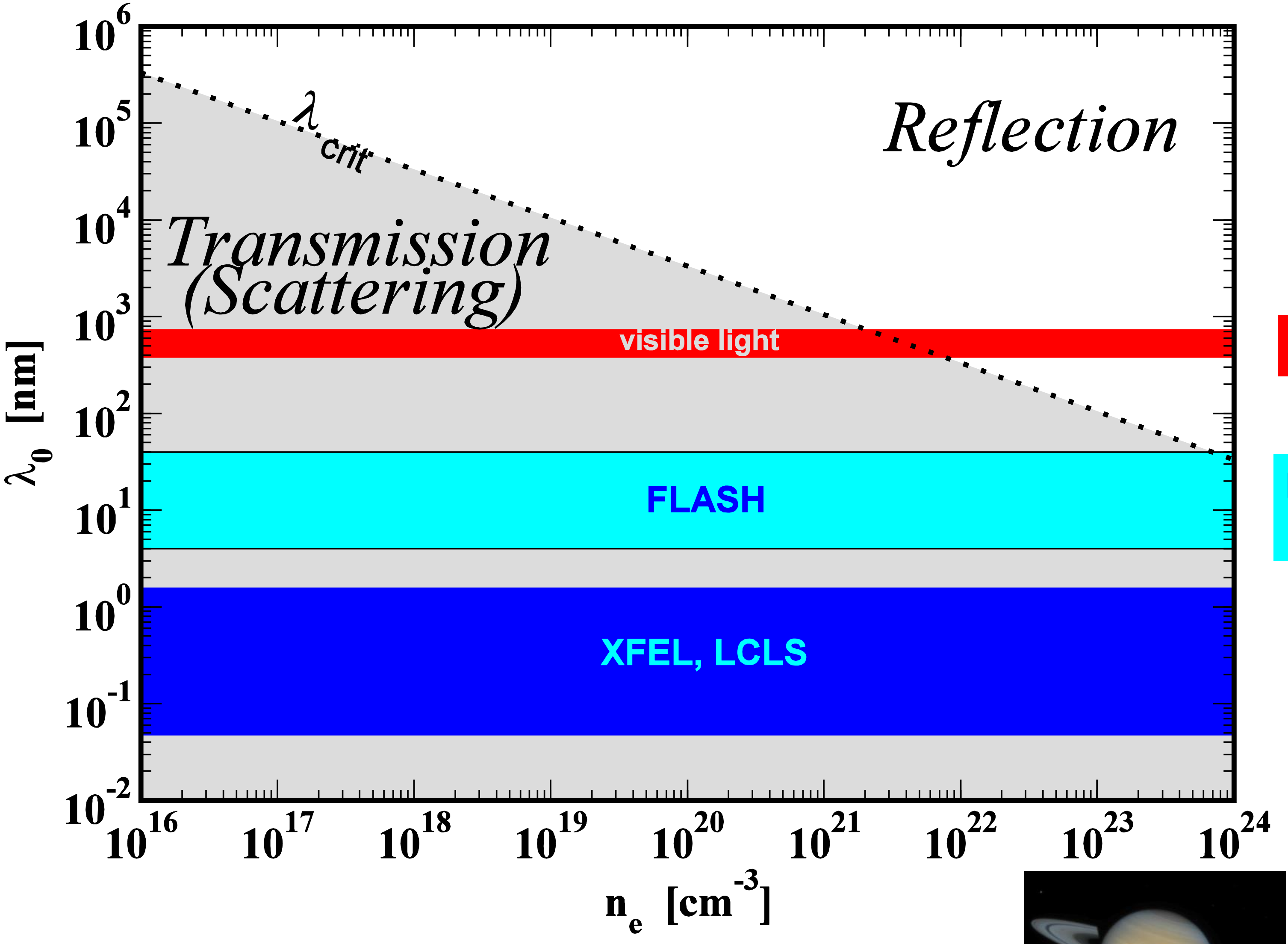

Ablation plasmas

Near-solid density plasmas

High-density plasmas

states deep in planetary interiors (eV and Mbar)

MEC @ LCLS, HED @ XFEL + HIBEF, HERMES @ SACLA; ESRF, PETRA III, APS

X-ray free-electron lasers worldwide with big OLs

The European XFEL will put Europe in the lead among industrialized nations in a highly competitive scientific and technical environment.

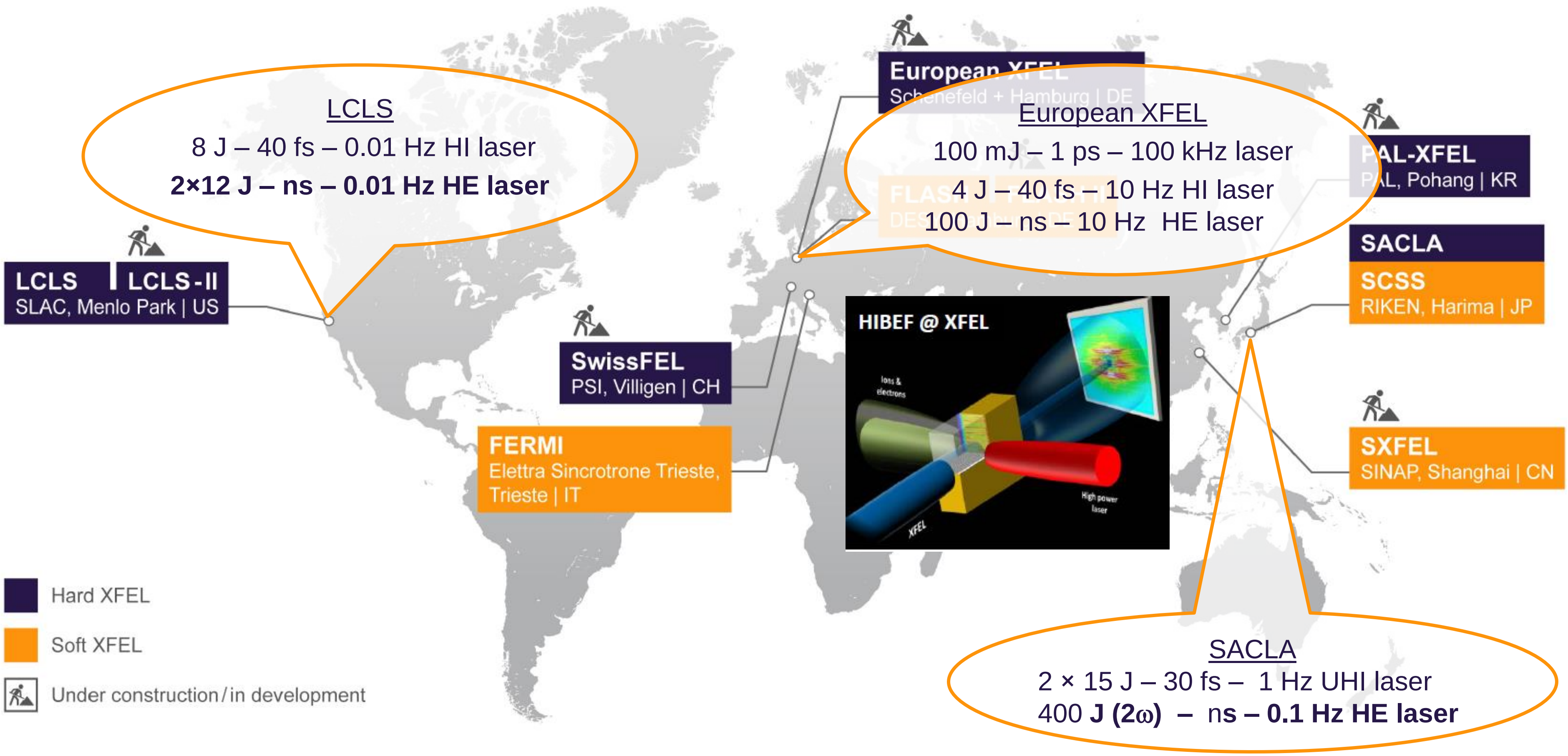

X-ray diagnostics

See M. McMahon, U. Zastrau:
CDR on HED experiments, Feb 2017

- **X-ray diffraction (XRD):** EOS, phase diagram
- **X-ray phase contrast imaging (PCI):** dynamics
- **X-ray absorption spectroscopy (XAS):** e-structure
- **X-ray near-edge absorption spectroscopy (XANES):** K and L edges
- **X-ray emission spectroscopy (XES):** Auger & radiative decays
- **X-ray Thomson scattering (XRTS)**
  non-collective (particles cattering)
  collective (plasmon scattering)
- **High-resolution inelastic X-ray scattering (hrIXS):** dynamic properties of solids and liquids

X-ray Thomson scattering (XRTS) in WDM

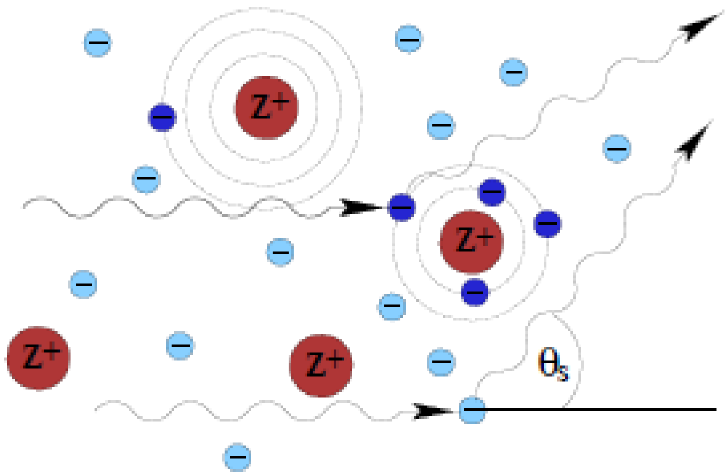

- free and bound electrons
- screening and correlation effects
- collisions between plasma particles

Scattering on density fluctuations: scattering parameter α

$$\alpha = \frac{1}{k\lambda_D} \begin{cases} < 1 & \text{thermal electron motion (non-collective)} \\ > 1 & \text{collective effects} \end{cases}$$

$\rightsquigarrow$ with $\lambda_D = \sqrt{\epsilon_0 k_B T_e / n_e\, e^2}$ and $k = 4\pi \sin(\theta_S/2)/\lambda_0$

S.H. Glenzer, RR, Rev. Mod. Phys. **81**, 1625 (2009)
E.E. Salpeter, Phys. Rev. **120**, 1528 (1960)

Theory for the XRTS spectrum

Dynamic structure factor $S_{ee}(k,\omega)$

Scattered power P_s into frequency interval $\omega \to \omega + d\omega$ and solid angle $d\Omega$ per time, measured by a detector located at $\vec{R}$

$$P_s(\vec{R},\omega)d\Omega d\omega = \frac{P_i r_0^2 d\Omega}{2\pi A}\left|\hat{\vec{k}}_f \times (\hat{\vec{k}}_f \times \hat{\vec{E}}_{0i})\right|^2 N S_{ee}(\vec{k},\omega)d\omega$$

- $r_0 = \frac{e^2}{m_e c^2}$: classical electron radius
- N: number of scattering centers, A: irradiated plasma spot size
- $\left|\hat{\vec{k}}_f \times (\hat{\vec{k}}_f \times \hat{\vec{E}}_{0i})\right|^2$: geometrical factor due to laser polarization
- $S_{ee}(\vec{k},\omega)$: dynamic structure factor (DSF), spectral function of the (electron) density fluctuations in the plasma, accessible via
  - X-ray Thomson scattering experiments
  - Theory for the dielectric function $\epsilon(\vec{k},\omega)$: fluctuation-dissipation theorem
  - Integral equation methods: HNC and classical-map HNC
  - *Ab initio* simulations: DFT-MD, WPMD

Chihara formula

$$S_{ee}(k,\omega) = Z_f S^0_{ee}(k,\omega) + |f_i(k) + q(k)|^2 S_{ii}(k,\omega) + Z_b \int_{-\infty}^{\infty} d\omega' S_c(k,\omega-\omega') S_s(k,\omega')$$

J. Chihara, J. Phys.: Cond. Matt. **12**, 231 (2000)
G. Gregori et al., Phys. Rev. E **67**, 026412 (2003)
A. Höll et al.. HEDP **3**, 120 (2007)

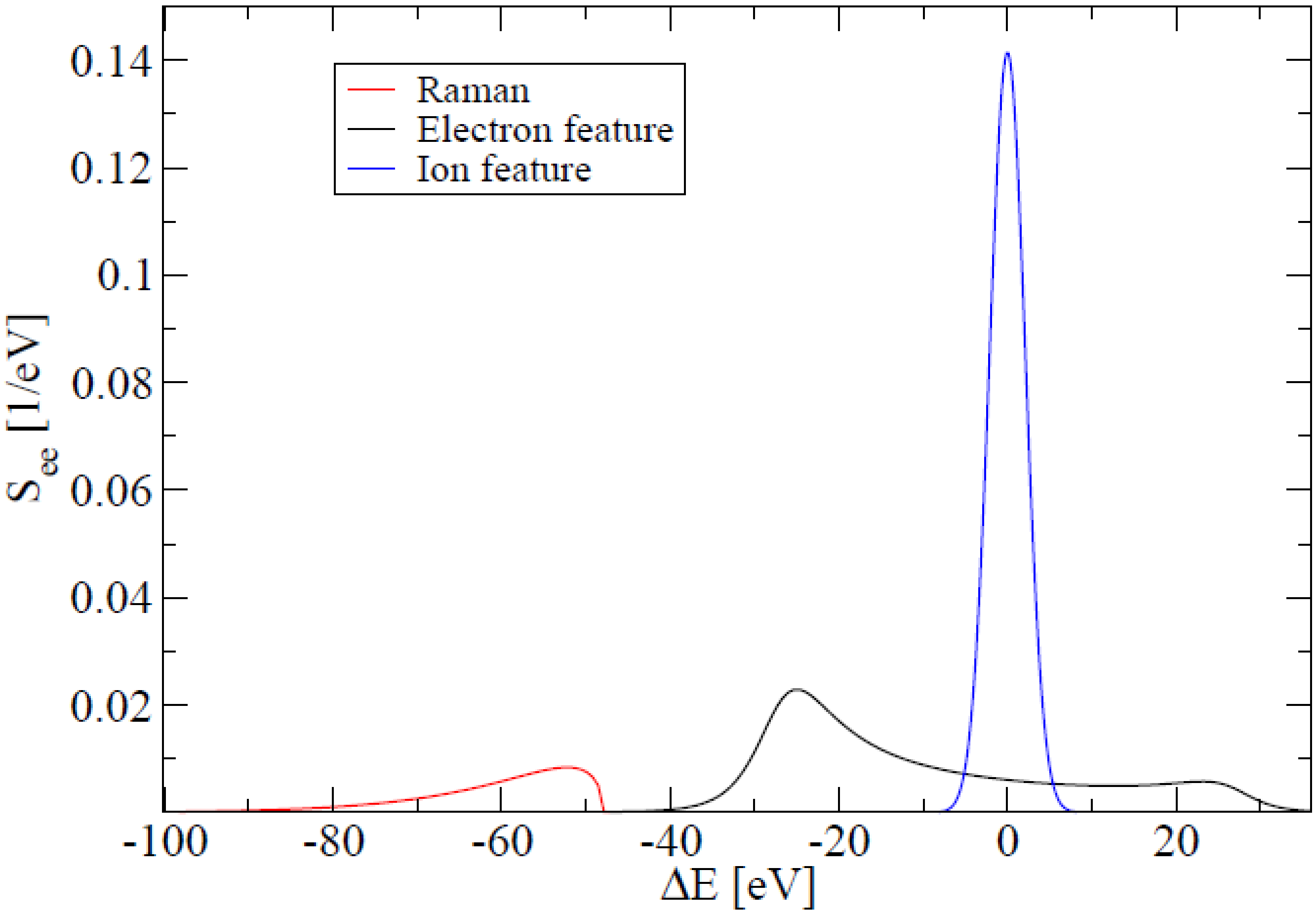

Born-Mermin approximation (BMA) [1,2]

- Fluctuation-dissipation theorem [3]: $$S^0_{ee}(k,\omega) = -\frac{\epsilon_0 \hbar k^2}{\pi e^2 n_e} \frac{\mathrm{Im}\,\epsilon^{-1}(k,\omega)}{1-\exp\left(-\hbar\omega/k_B T_e\right)}$$

- Collisions via Mermin ansatz [4]: $$\epsilon^M(k,\omega) - 1 = \frac{\left(1 + i\frac{\nu(\omega)}{\omega}\right)\left[\epsilon^{RPA}(k,\omega+i\nu(\omega)) - 1\right]}{1 + i\frac{\nu(\omega)}{\omega}\frac{\epsilon^{RPA}(k,\omega+i\nu(\omega))-1}{\epsilon^{RPA}(k,0)-1}}$$

- RPA given by Lindhard [5]: $$\epsilon^{RPA}(\vec{k},\omega) = 1 - \frac{1}{\Omega_0 \epsilon_0 k^2}\sum_{p,c} e_c^2 \frac{f^c_{p+(k/2)} - f^c_{p-(k/2)}}{\Delta E^c_{p,k} - \hbar(\omega + i\eta)}$$

- Dynamic collision frequency in Born approximation [6]:

$$\nu^{Born}(\omega) = -i\frac{\epsilon_0 n_i \Omega_0^2}{6\pi^2 e^2 n_e m_e}\int_0^\infty dq\, q^6 V_D^2(q) S_{ii}(q) \frac{1}{\omega}\left[\epsilon_{RPA}(q,\omega) - \epsilon_{RPA}(q,0)\right]$$

[1] R. Redmer, H. Reinholz, G. Röpke, R. Thiele, A. Höll, IEEE Trans. Plasma Sci. **33**, 77 (2005)
[2] C. Fortmann *et al.*, Laser Part. Beams **27**, 311 (2009)
[3] G.D. Mahan, *Many-Particle Physics* (Plenum Publishers, New York, 2000)
[4] N.D. Mermin, Phys. Rev. B **1**, 2362 (1970)
[5] J. Lindhard, Kgl. Dan. Videns. Selk. Mat. Fys. Medd. **28**, 8 (1954)
[6] H. Reinholz, R. Redmer, G. Röpke, A. Wierling, Phys. Rev. E **62**, 5648 (2000)

→ collisionality
→ conductivity

Electron DSF $S_{ee}^0(k,\omega)$

Hydrogen plasma: $n_e=10^{21}$ cm^{-3}, $\lambda_0=4.13$ nm, Z=1

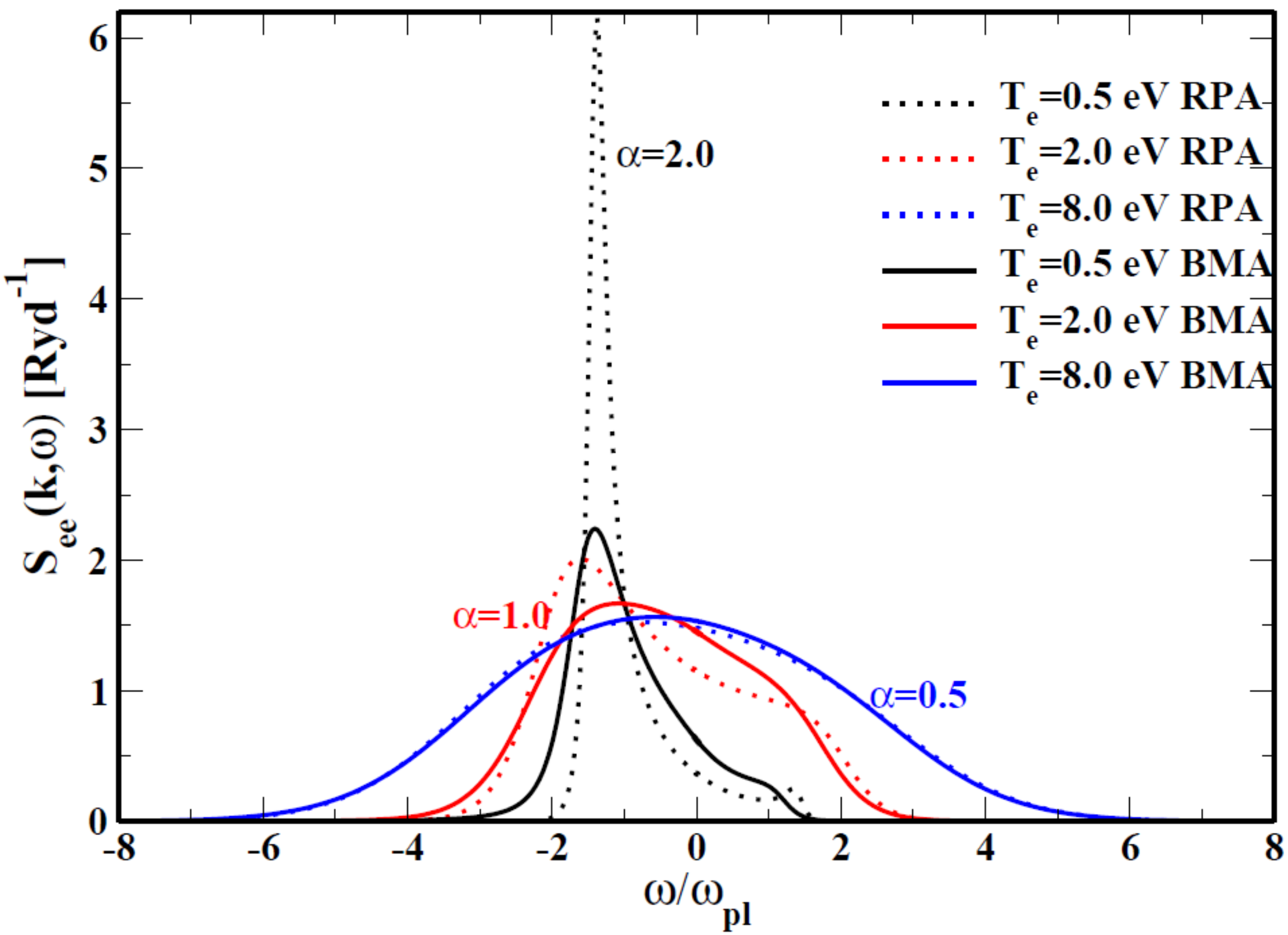

G. Gregori et al., Phys. Rev. E **67**, 026412 (2003)
A. Höll et al., High Energy Dens. Phys. **3**, 120 (2007)
R. Thiele et al., Phys. Rev. E **78**, 026411 (2008)

Collective XRTS: plasmons

T_e via detailed balance relation:

$$Y(\mathbf{k},\omega) = \frac{S^0_{ee}(-\mathbf{k},-\omega)}{S^0_{ee}(\mathbf{k},\omega)} = \exp\left(-\frac{\hbar\omega}{k_B T_\mathrm{e}}\right)$$

Peak positions give n_e:

$$\omega^2_{\mathrm{GB}}(k) = \omega^2_{pl} + \frac{3k_B T_e}{m_e}k^2$$

Gross-Bohm (1949)

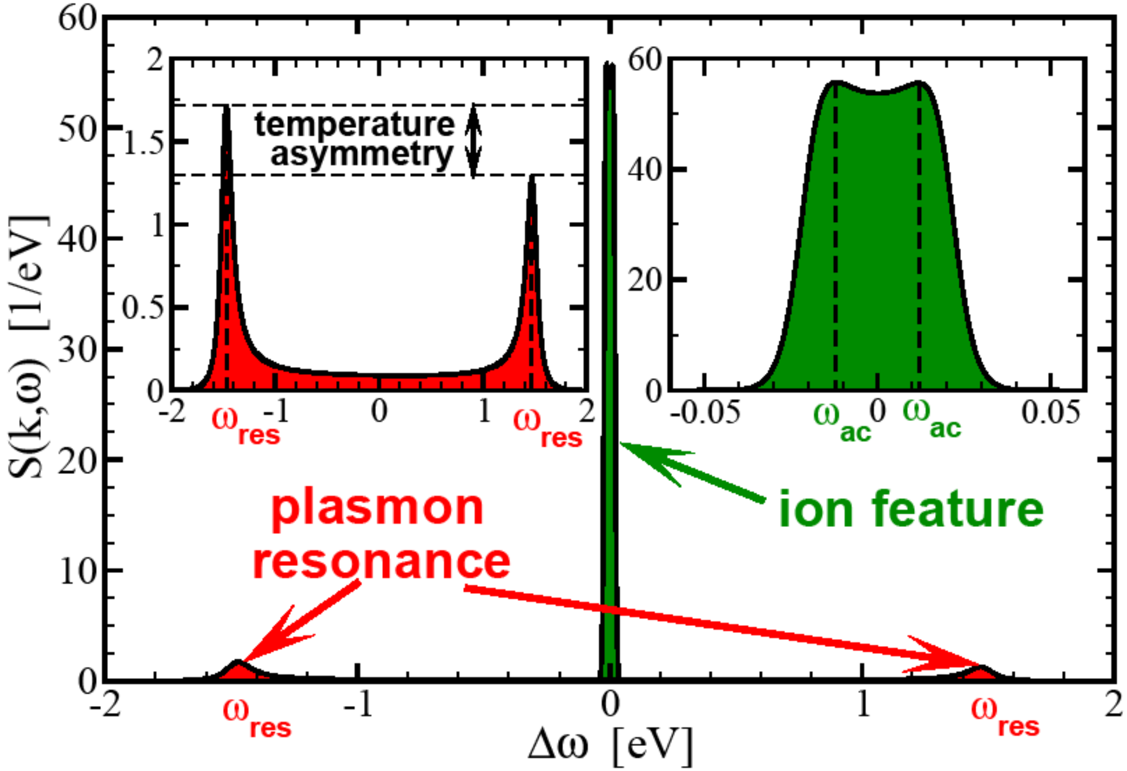

A. Höll et al., High Energy Dens. Phys. **3**, 120 (2007)
R. Thiele et al., Phys. Rev. E **78**, 026411 (2008)
S.H. Glenzer, RR, Rev. Mod. Phys. **81**, 1625 (2009)

Collective XRTS: Be

Plasmon feature

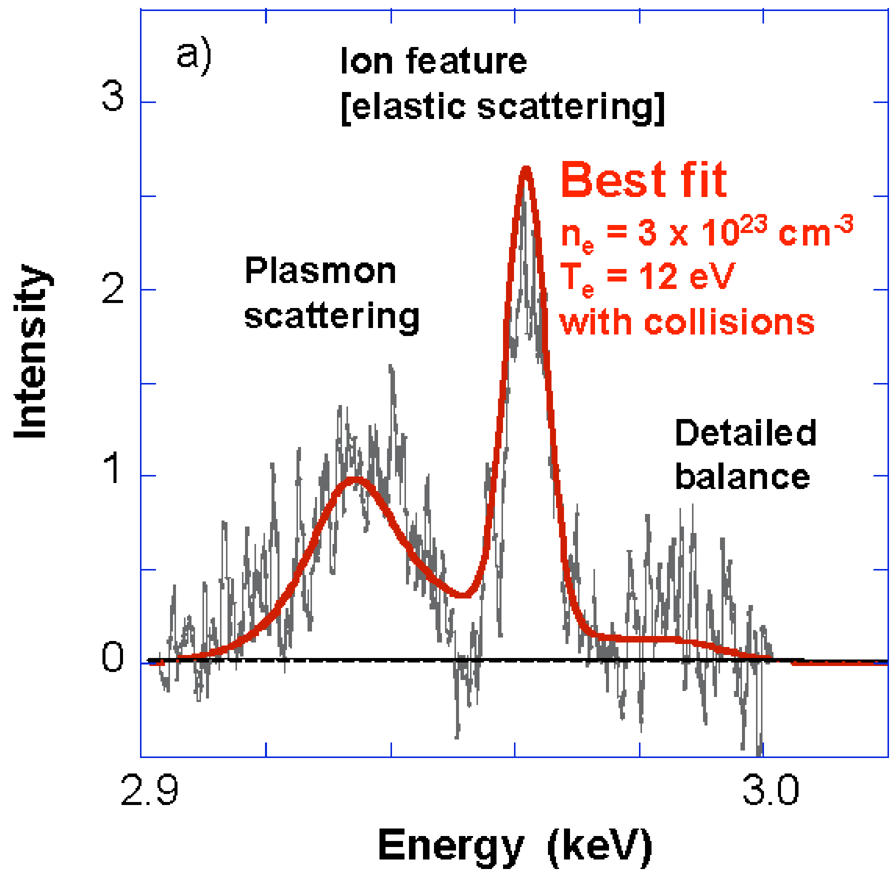

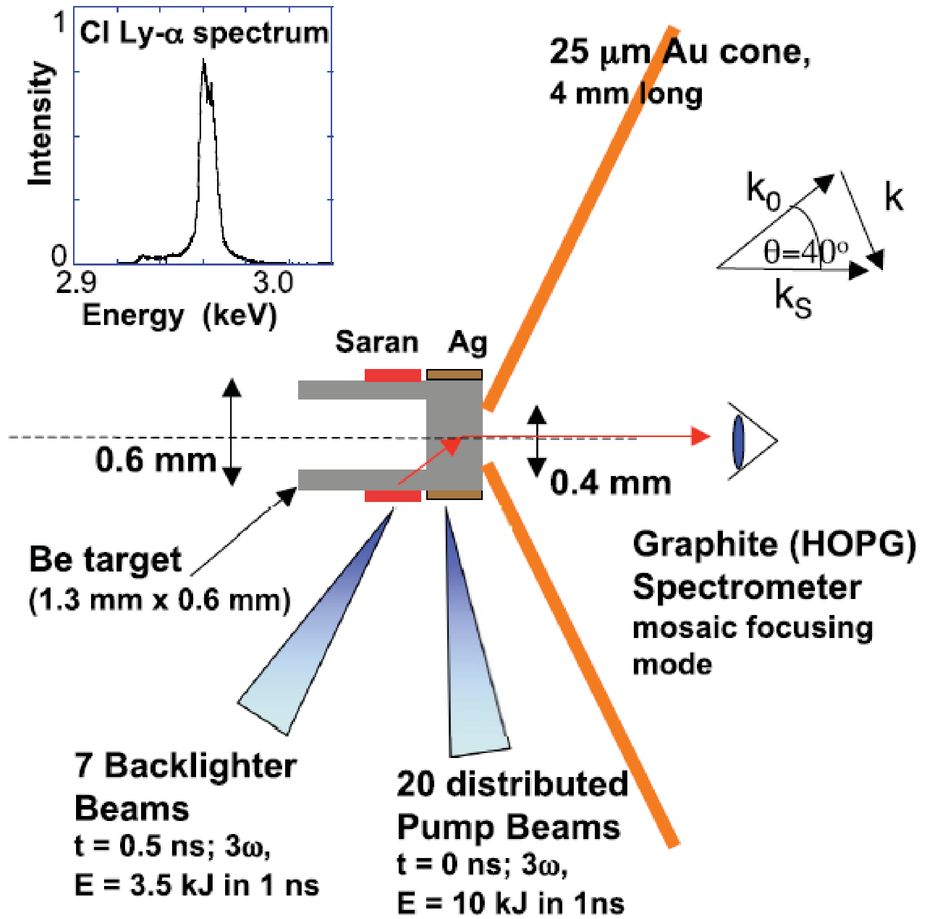

Experiment at the Omega laser facility in Rochester:
S.H. Glenzer et al., Phys. Rev. Lett. **98**, 065002 (2007)

Pump-probe XRTS experiment: LiH

ns time resolution, nonmetal-to-metal transition

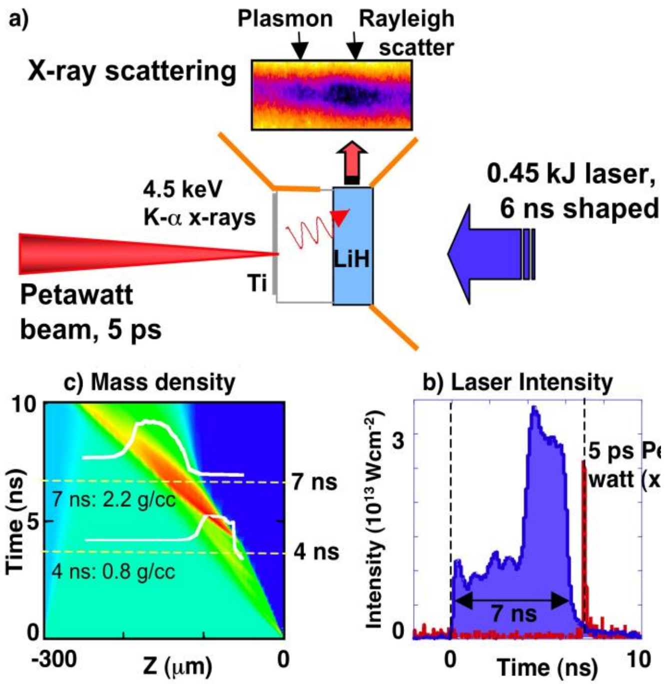

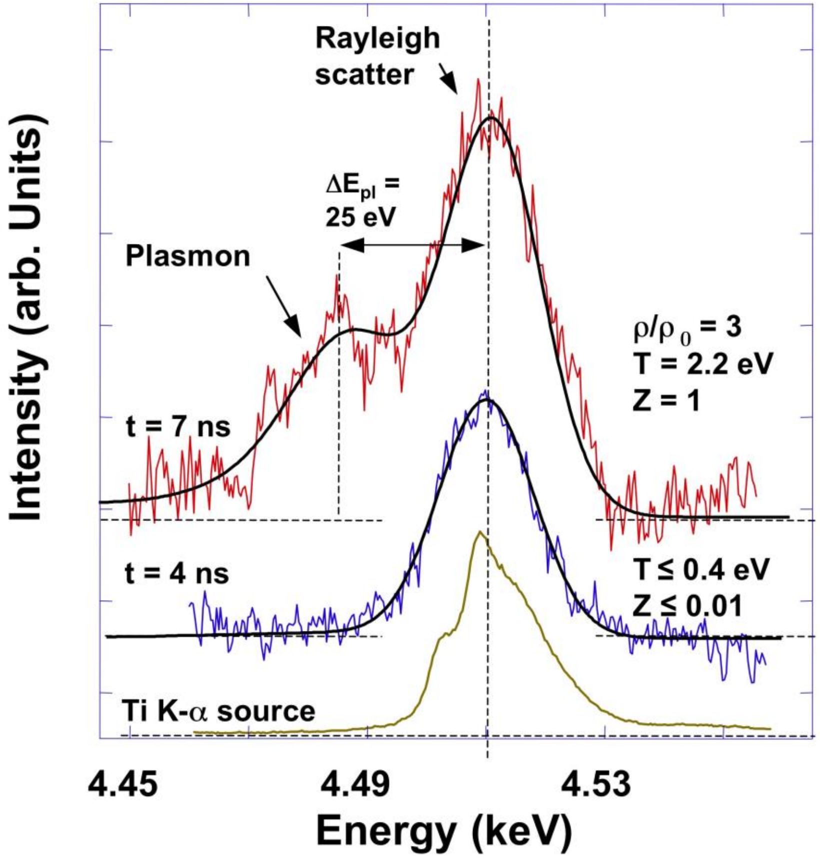

Experiment at the Titan laser facility at LLNL:
A. Kritcher et al., Science **322**, 69 (2008); PoP **16**, 056308 (2009).

Pump-probe XRTS experiment: H

Probes onset of dissociation in Jupiter

P. Davis et al., Nature Commun. **7**, 11189 (2016)
Experiment at the Janus laser facility at LLNL
DFT-MD: A. Becker (U Rostock)

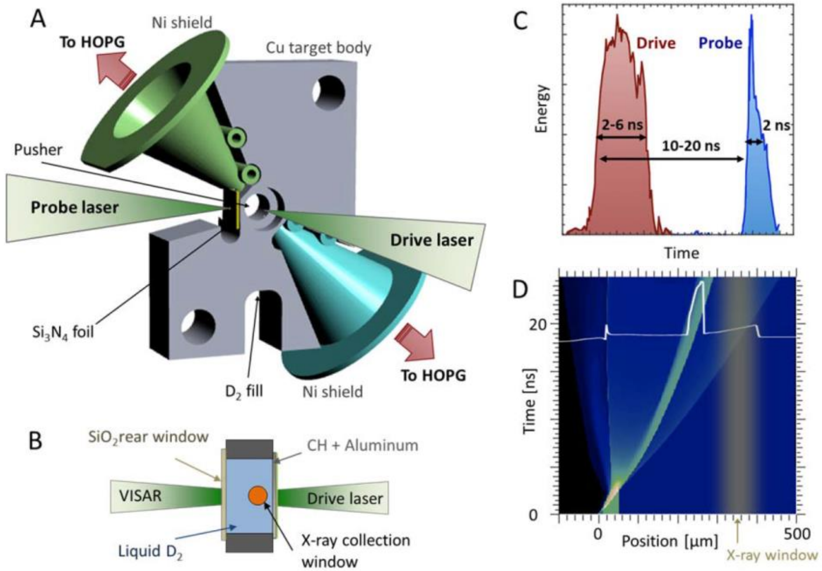

Probe: 2005 eV Si Lyman-α line

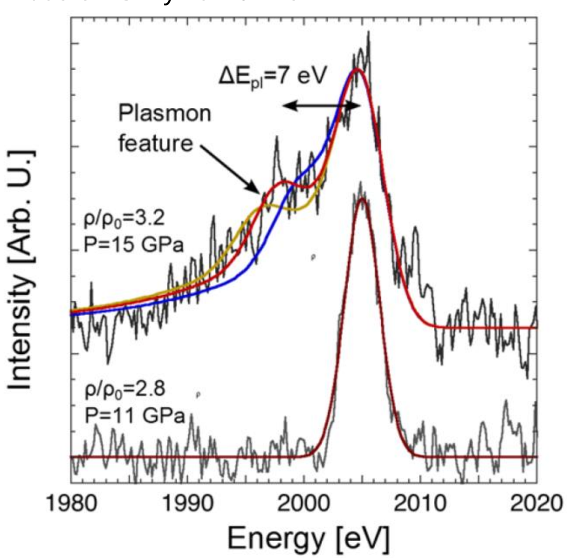

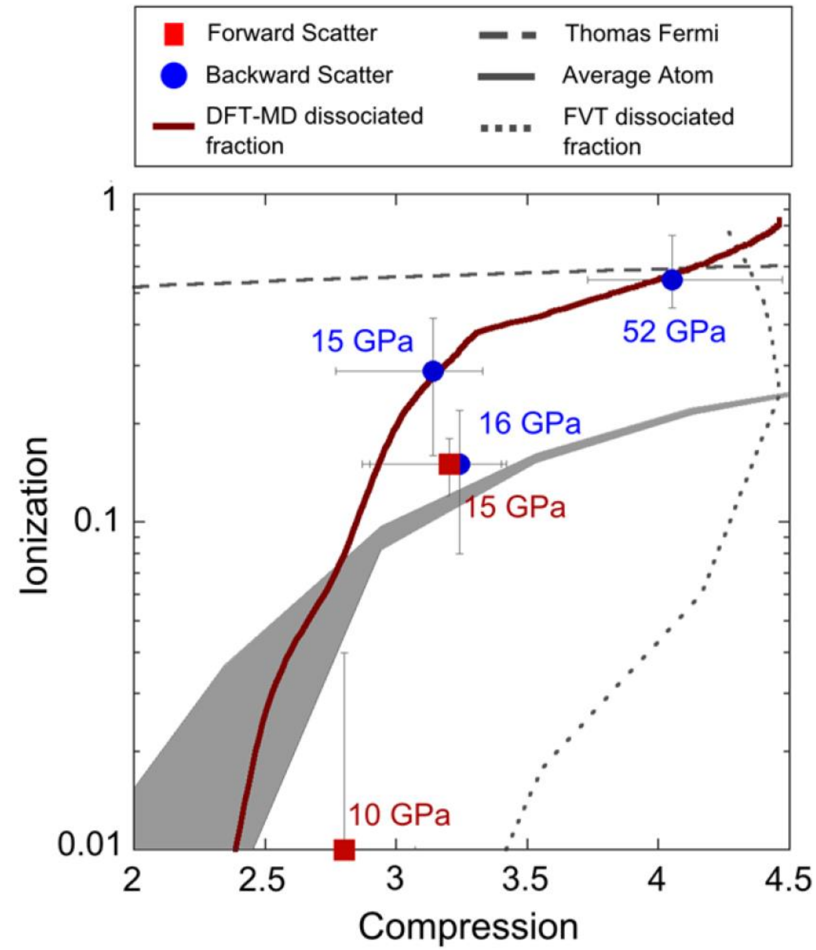

OL → XRTS at FELs

High peak brilliance

FLASH Hamburg
MEC@LCLS Stanford
FERMI@ELETTRA Trieste
HERMES@SACLA Harima
HED@European XFEL Schenefeld
& HIBEF Project
(opt. pump laser >100 J, 2-15 ns,
pulse shaping)

M. McMahon, U. Zastrau:
CDR on HED experiments, Feb 2017

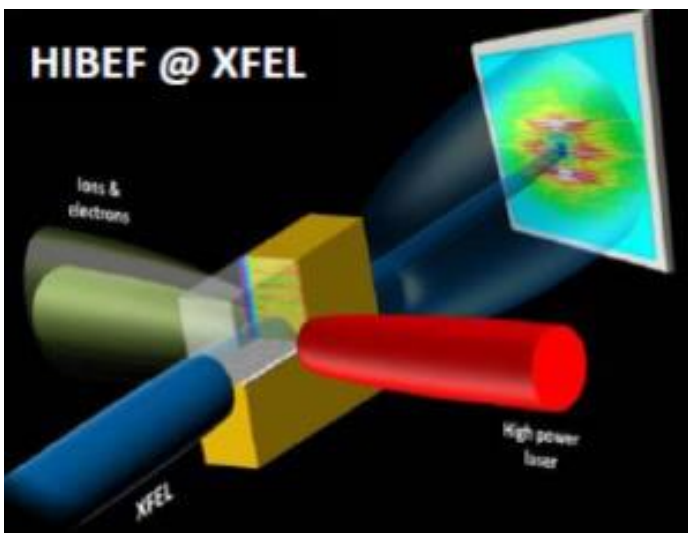

By courtesy of European XFEL

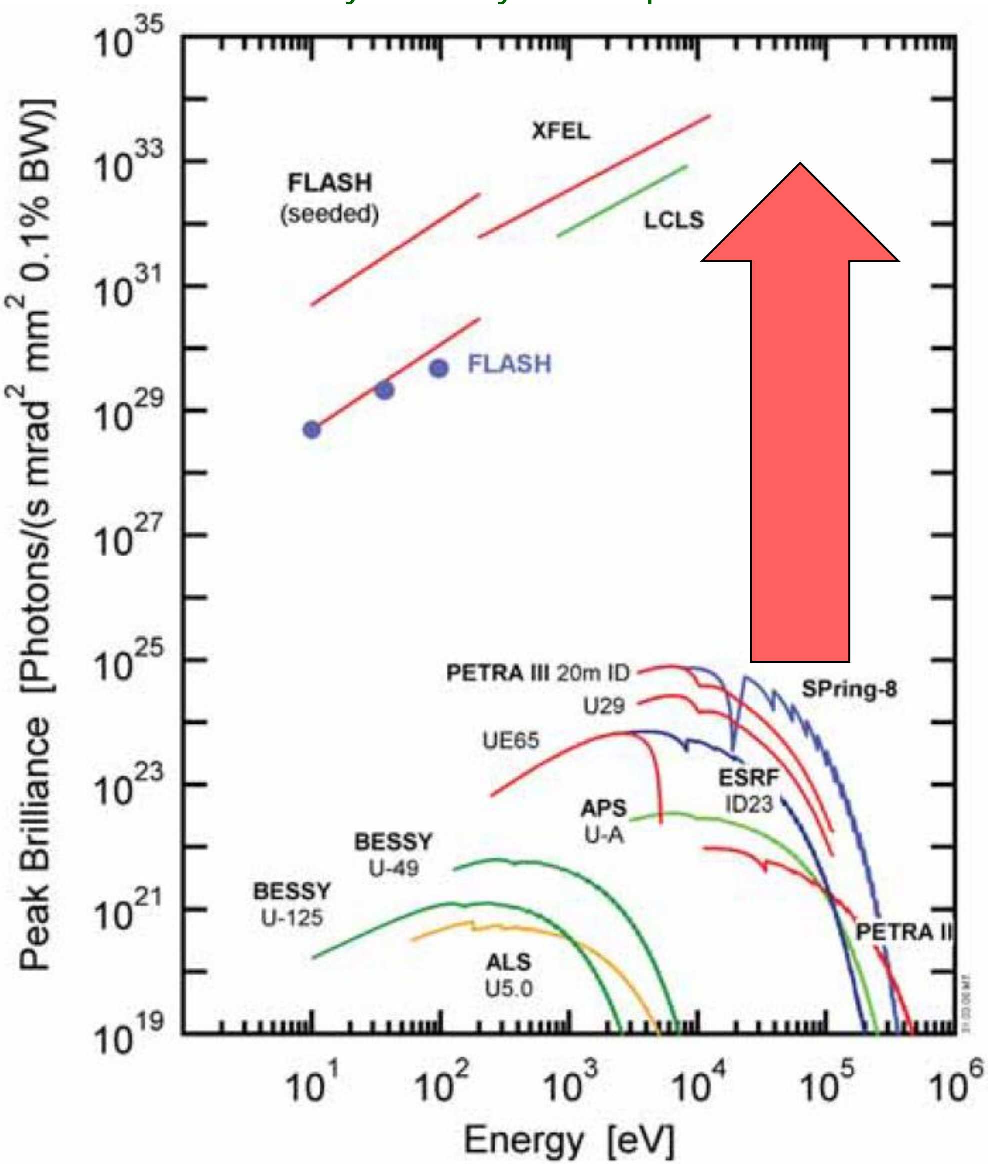

Pump-probe XRTS experiment: Al

High spectral resolution at LCLS (seeded beam mode)

Be: optical laser

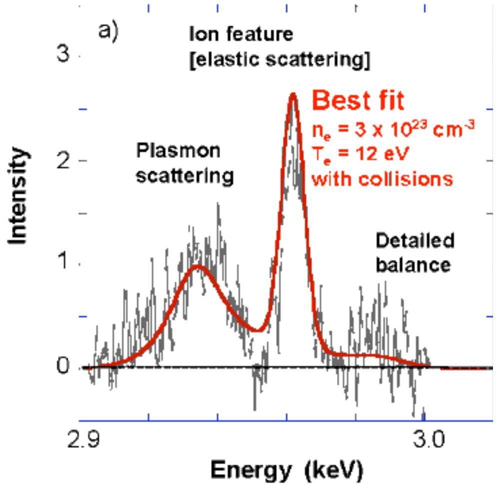

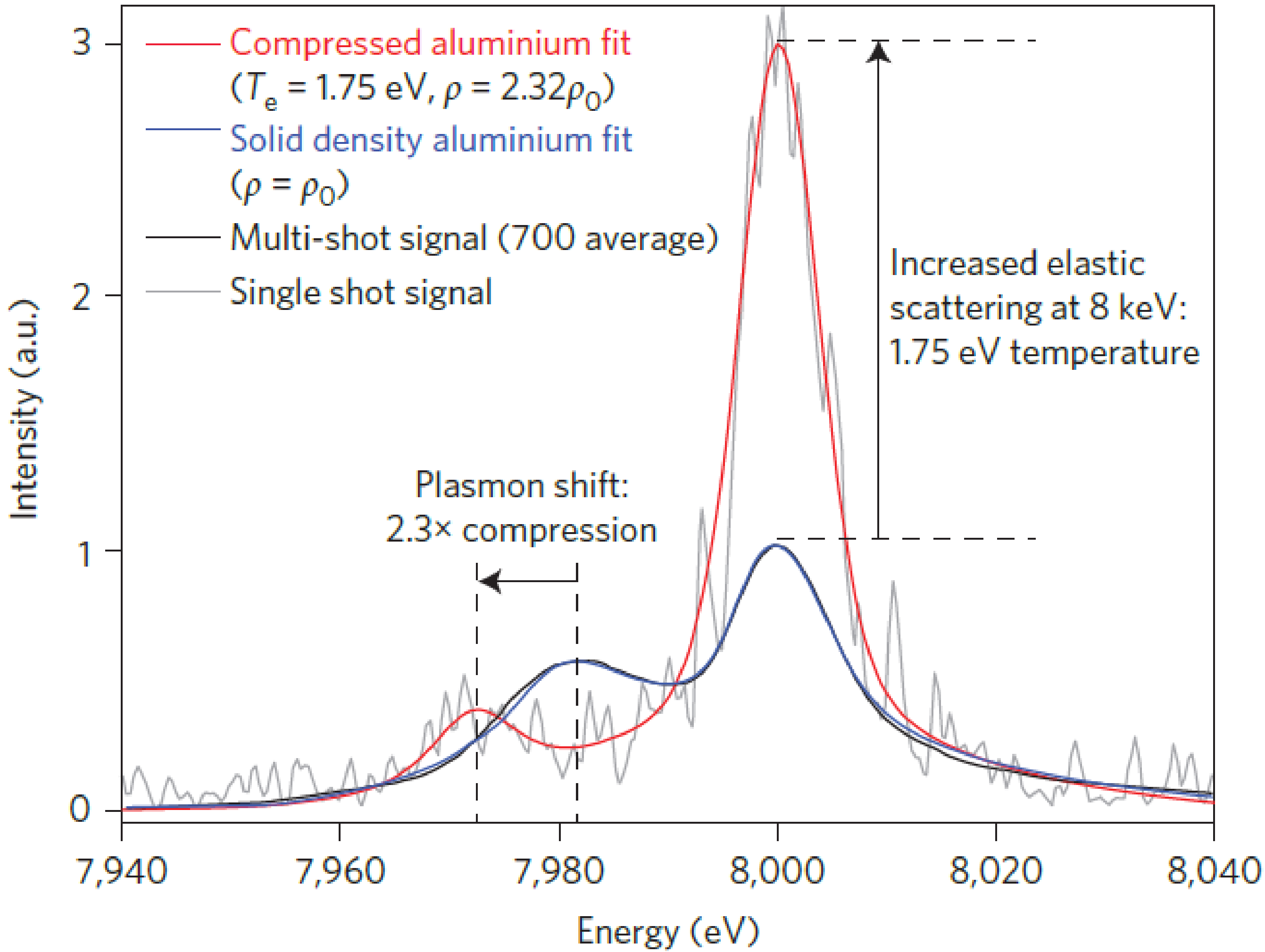

L.B. Fletcher et al., Nature Phot. **9**, 274 (2015)
Ion feature: DFT-MD → Yukawa+SRR S(k)
Plasmon feature: BMA and BMA+LFC

Contents

DFT-MD Simulations for WDM

Born-Oppenheimer approximation: combination of (quantum) DFT and (classical) MD
Warm Dense Matter: finite-temperature DFT-MD simulations based on
N.D. Mermin, Phys. Rev. **137,** A1441 (1965)
Codes: **Vienna Ab-initio Simulation Package** (VASP) or Abinit, Quantum Espresso …
G. Kresse and J. Hafner, PRB **47**, 558 (1993), ibid. **49**, 14251 (1994)
G. Kresse and J. Furthmüller, Comput. Mat. Sci. **6**, 15 (1996), PRB **54**, 11169 (1996)

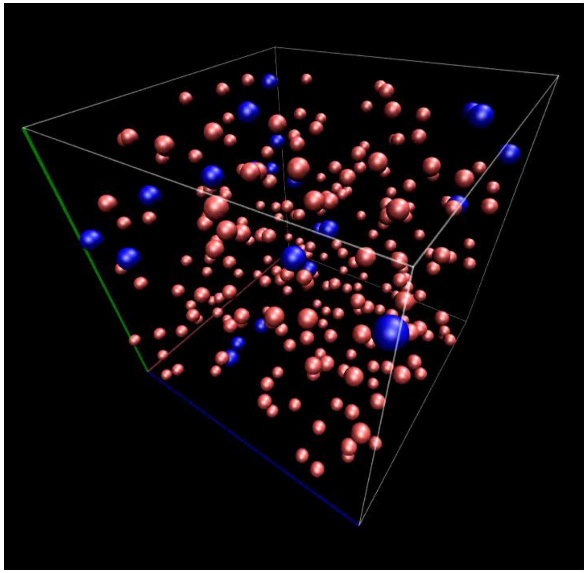

H-He (8.6%) @ 1 Mbar, 4000 K

box length ~ 10^{-9} m

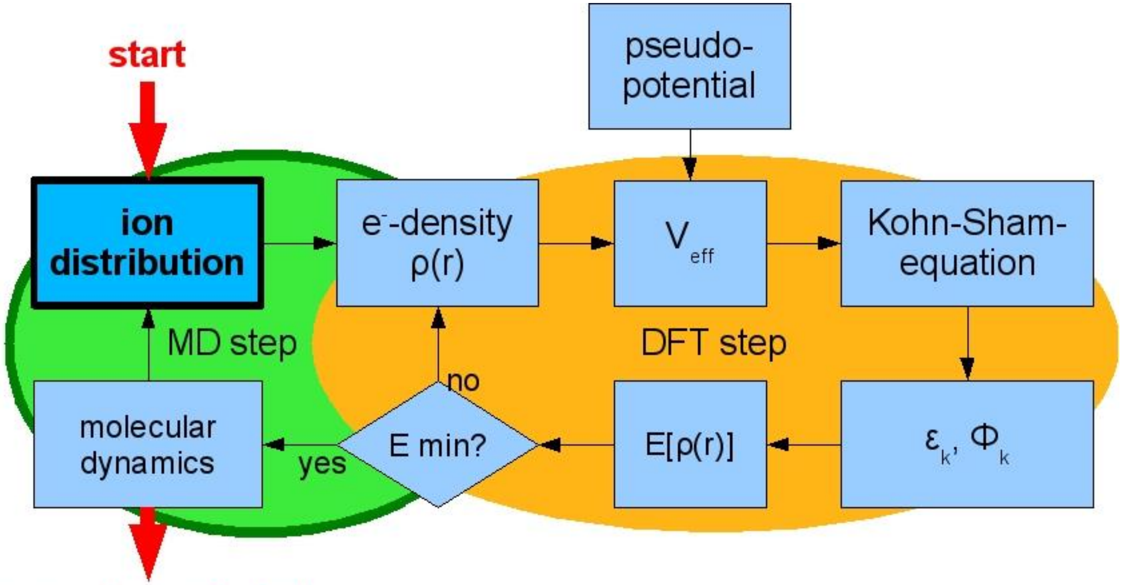

thermodynamic data
high-pressure phase diagram
pair correlation functions
electrical & thermal conductivity
diffusion coefficient
viscosity, opacity

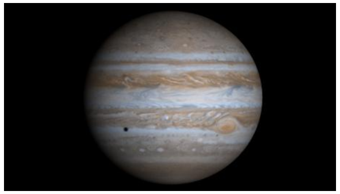

GP size ~ 10^8 m

Ion feature in warm dense Be

$$S_{ee}^{i}(\vec{k}) = |f(\vec{k}) + q(\vec{k})|^2 S_{ii}(\vec{k}) \equiv |N(\vec{k})|^2 S_{ii}(\vec{k}).$$

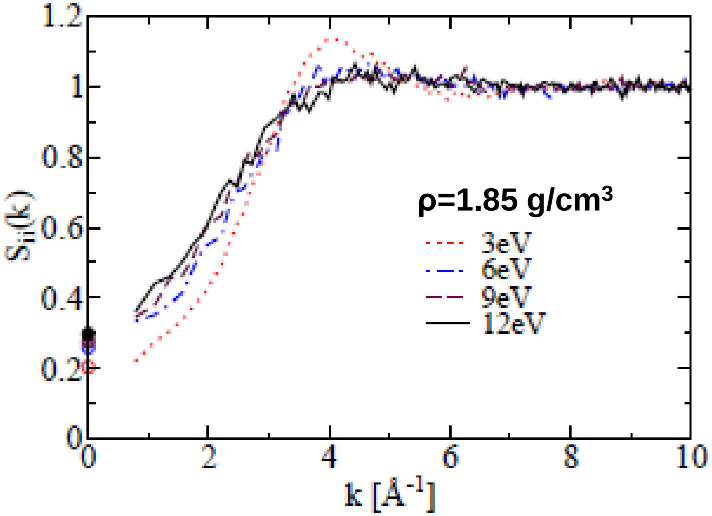

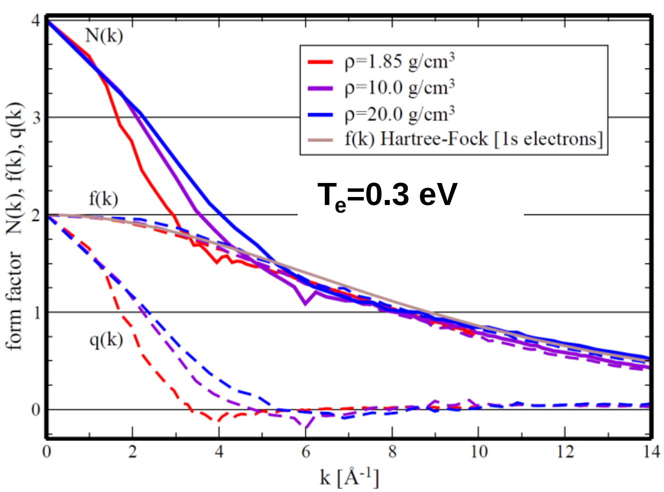

Warm dense Be:
12 eV, 1.85 g/cm³

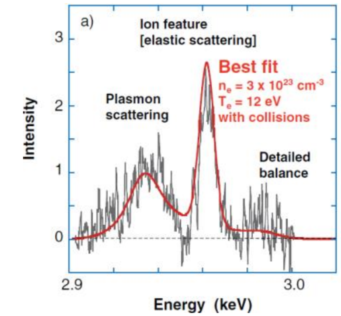

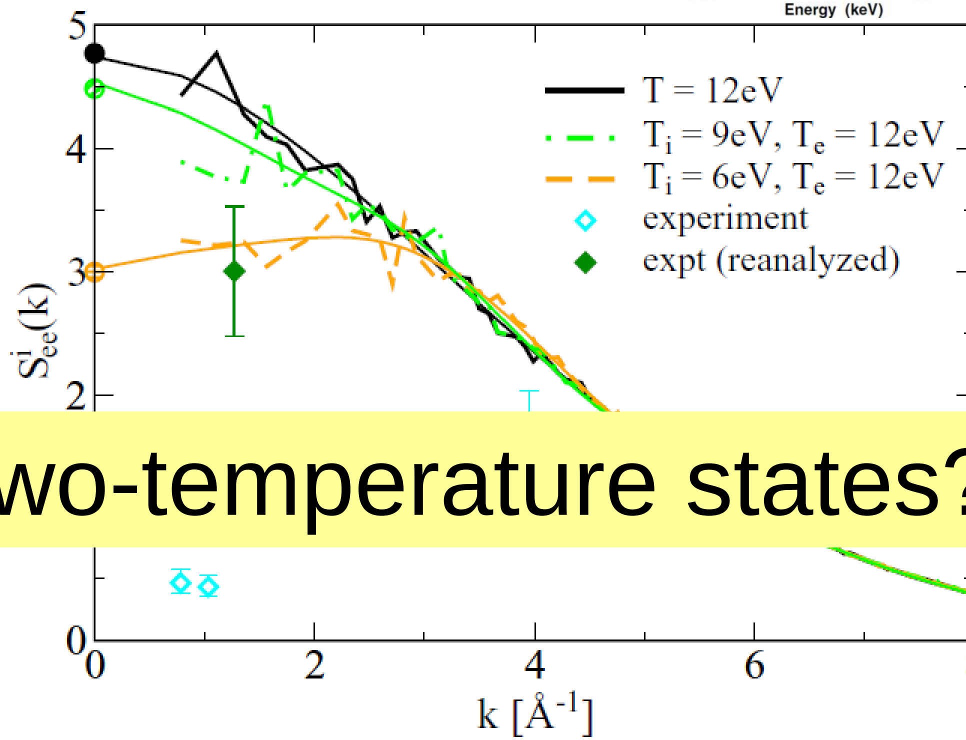

Two-temperature states?

Experiments: see Glenzer, RR, RMP **81**, 1625 (2009)
Reanalyzed spectrum from Glenzer et al., PRL **98**, 065002 (2007)
DFT-MD simulations: Plagemann et al., PRE **92**, 013103 (2015)

Pump-probe experiments at FLASH

Temporal resolution of ultrafast heating in liquid hydrogen on ps time scales.
2T-DFT-MD simulations for S(k→0) based on rad-hydro target evolution.

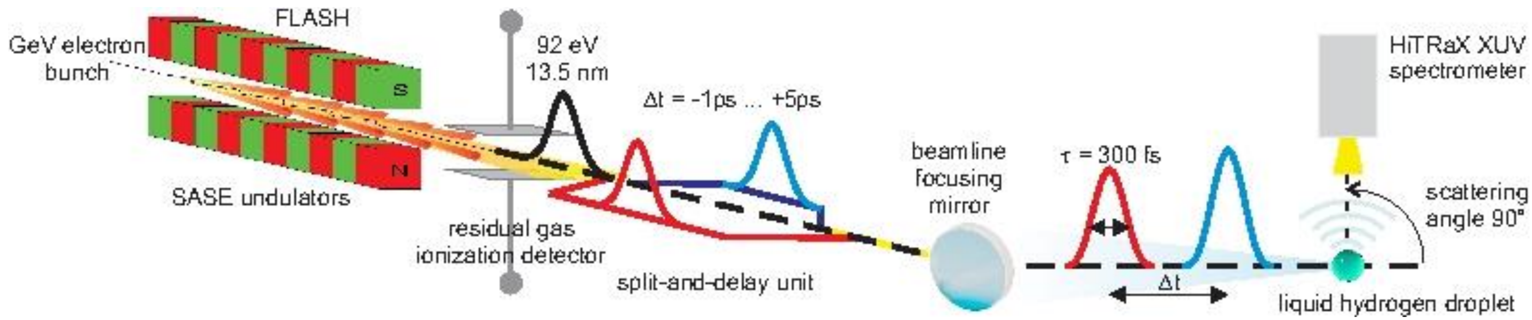

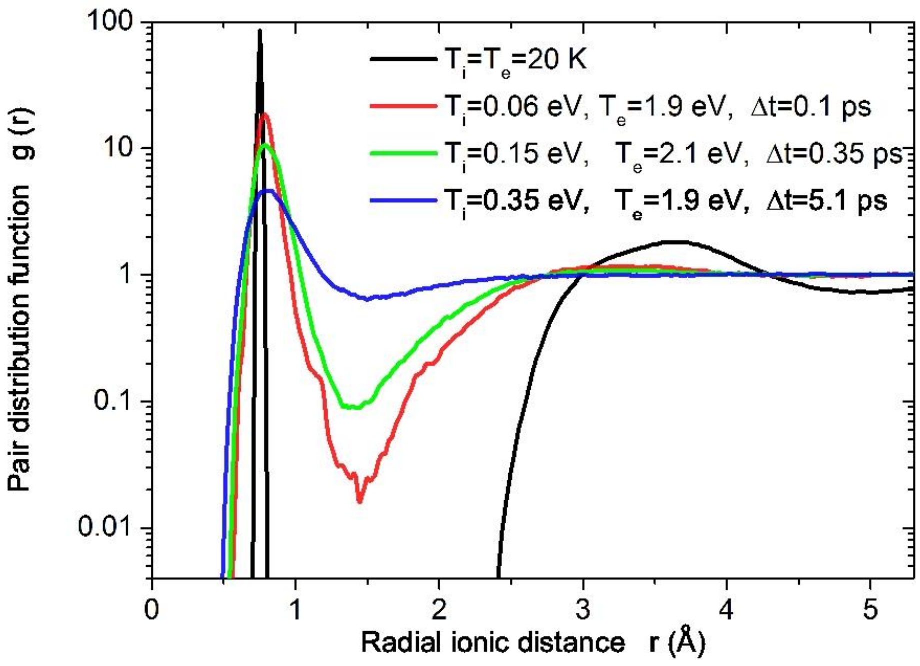

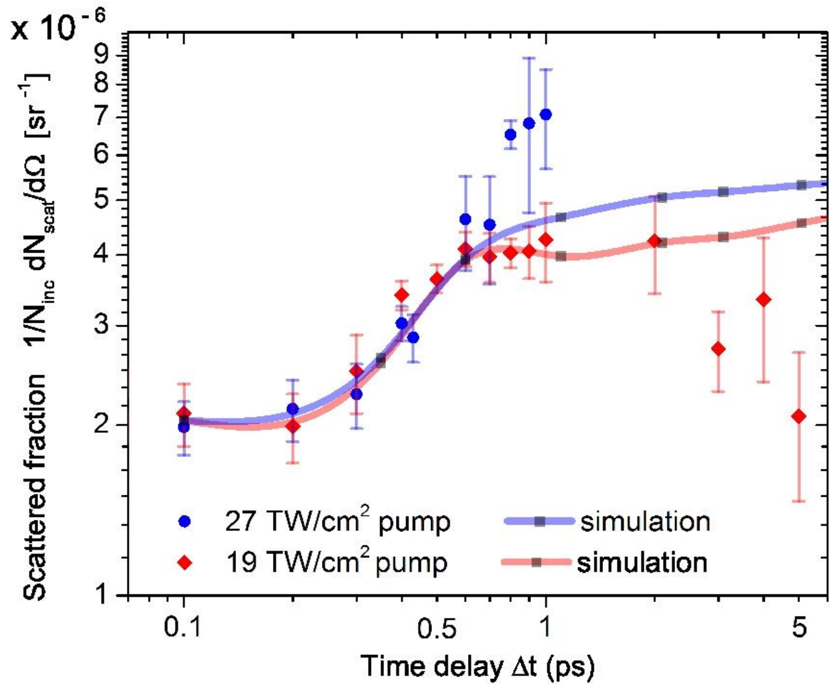

U. Zastrau, P. Sperling et al., PRL **112**, 105002 (2014)

XRTS for inhomogeneous plasmas

State-of-the-art experiments combine optical lasers (pump) and XFELs (probe).
Interpret the XRTS signal of a strongly inhomogeneous plasma?
Perform PIC (VLPL3D) and hydrodynamic simulations (HELIOS) for laser-matter interaction.
Study the ultra-fast dynamics and relaxation in inhomogeneous plasmas!

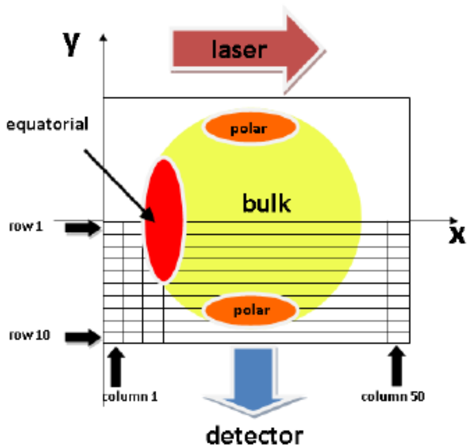

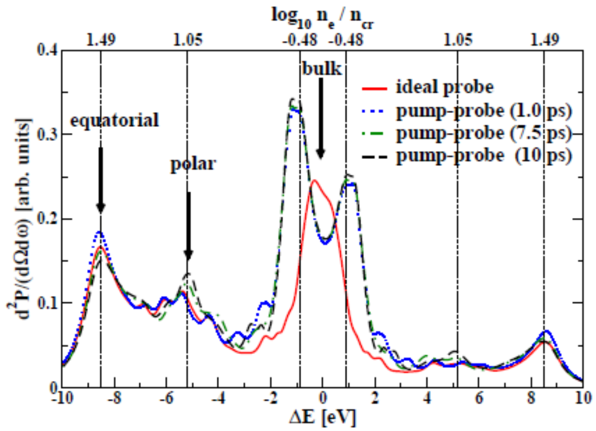

OL:
800 nm
150 fs
1.6 mJ
XFEL:
13.5 nm
30 fs
0.05 mJ
Target:
liquid H
15 μm

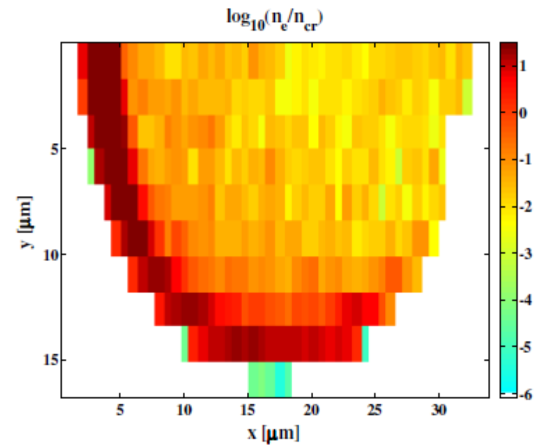

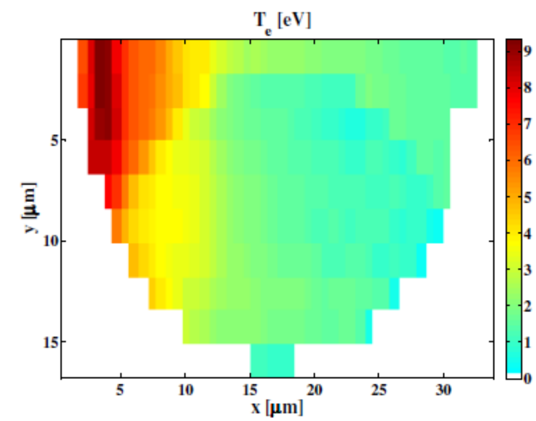

R. Thiele et al., PRE **82**, 056404 (2010)

Next step: derive all relevant quantities from DFT-MD

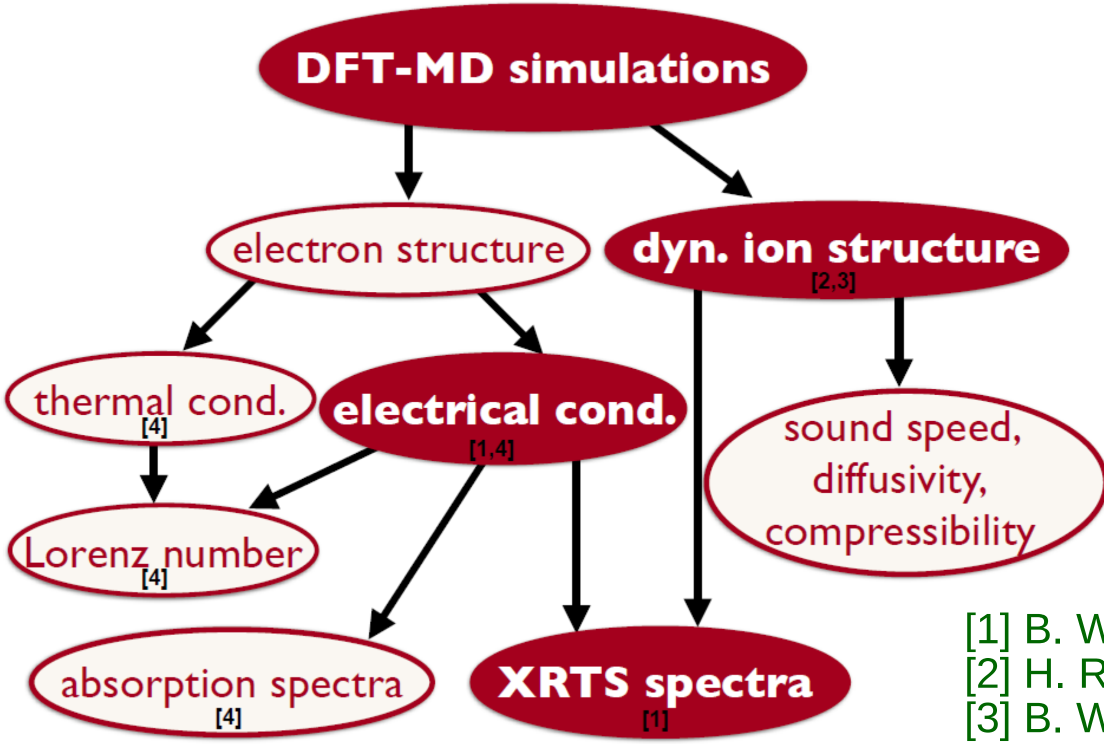

[1] B. Witte et al., PRL **118**, 225001 (2017)
[2] H. Rüter, RR, PRL **112**, 145007 (2014)
[3] B. Witte et al., PRB **95**, 144105 (2017)
[4] B. Witte et al., PoP **25**, 056901 (2018)

DSF & XRTS spectrum exclusively from DFT-MD

$$S_{ee}(k,\omega) = \underbrace{|f_I(k)+q(k)|^2}_{|\Psi_{\mathbf{k}}|^2\ [3]} \underbrace{S_{ii}(k,\omega)}_{\langle n_k(0) n_{-k}(t)\rangle\ [2]} + \underbrace{S_{\mathrm{et}}(k,\omega)}_{|<\Psi_{\mathbf{k}}|\hat{\mathrm{p}}|\Psi_{\mathbf{k}}>|^2\ [1]}$$

XRTS in isochorically heated Al

measured XRTS spectrum

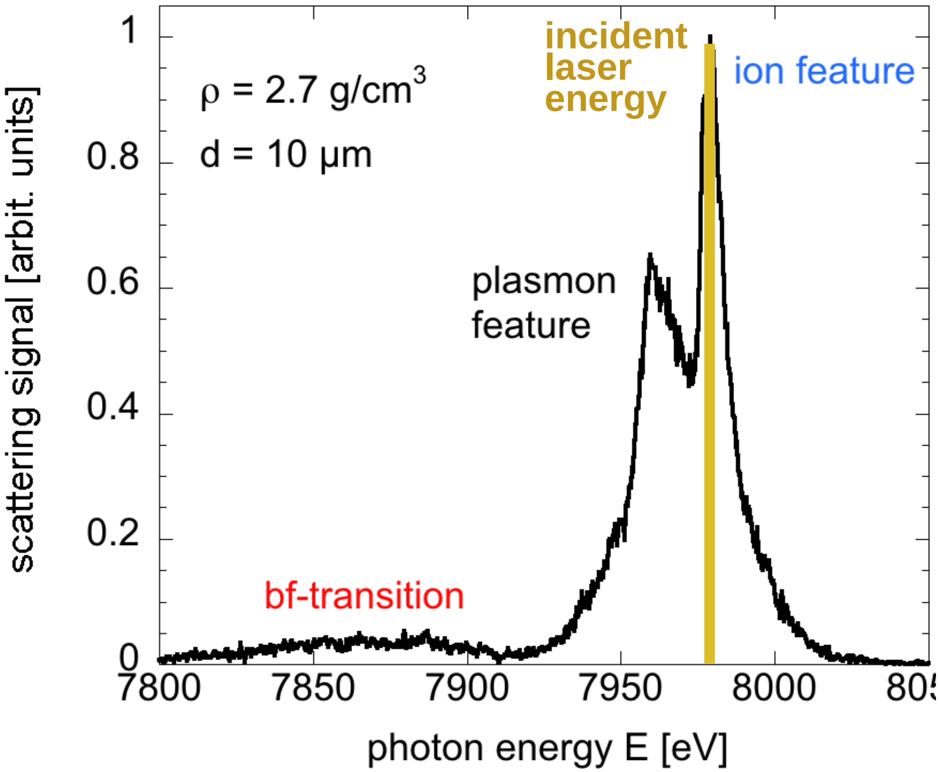

standard theory fails

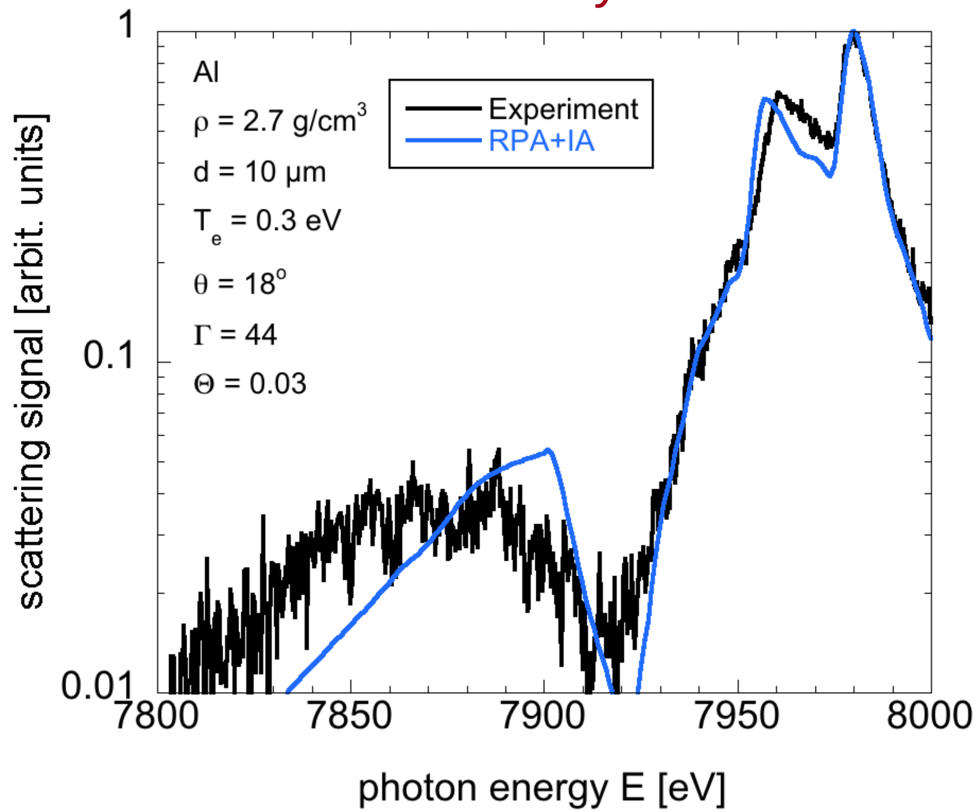

Highly resolved XRTS spectrum of 50 μm thick Al foils averaged over 10^3-10^4 shots at LCLS → challenges theory for the DSF and the dielectric function

P. Sperling et al., PRL **115**, 115001 (2015)
B. Witte et al., PRL **118**, 225001 (2017)

XRTS in isochorically heated Al

$$\sigma_e(\omega) \propto \sum_{\mathbf{k}\mu\nu} (f_{\mathbf{k}\mu} - f_{\mathbf{k}\nu}) \left|\langle \Psi_{\mathbf{k}\nu} | \hat{\mathbf{p}} | \Psi_{\mathbf{k}\mu} \rangle\right|^2 \delta(\Delta\epsilon_{\mathbf{k}\nu\mu} - \hbar\omega)$$

See B. Holst, M. French, RR, PRB 83 (2011)

Simple Drude model:

$$\sigma(\omega) = \frac{\epsilon_0 \nu \omega_{pl}^2}{\omega^2 + \nu^2}$$

XC functional matters: PBE, HSE

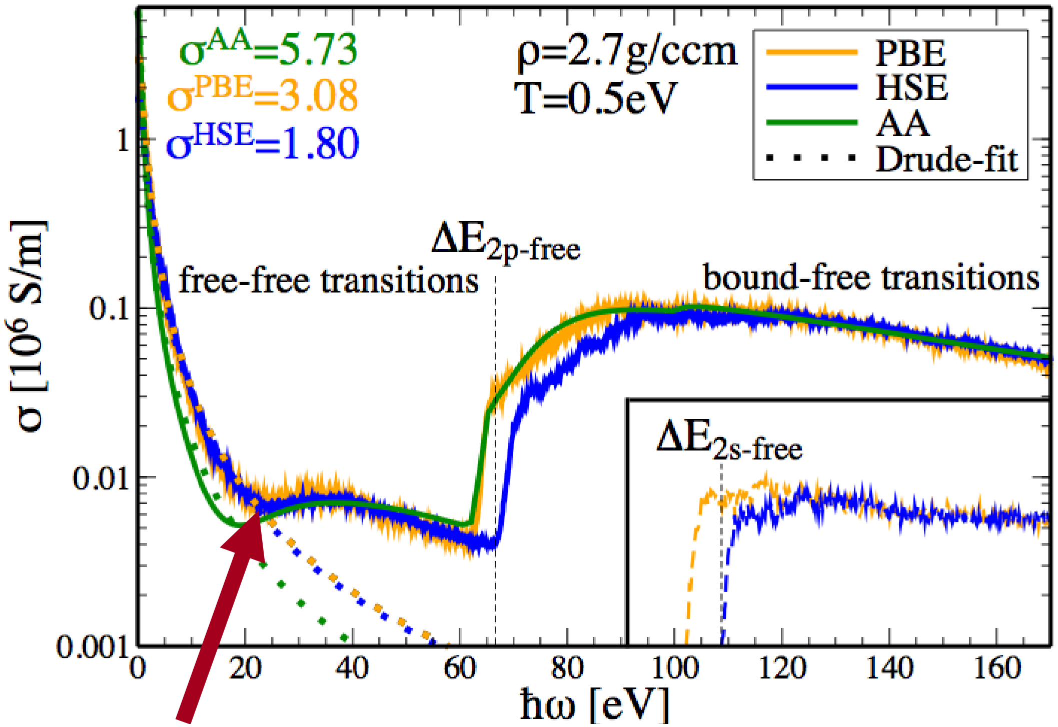

Cooper minimum: non-Drude behavior

DSF → XRTS spectrum:

$$\mathrm{Re}\,\epsilon(\omega) = 1 - \frac{1}{\epsilon_0 \omega} \mathrm{Im}\,\sigma(\omega),$$

$$\mathrm{Im}\,\epsilon(\omega) = \frac{1}{\epsilon_0 \omega} \mathrm{Re}\,\sigma(\omega).$$

$$S^0_{\mathrm{ee}}(k,\omega) = -\frac{\epsilon_0 \hbar k^2}{\pi e^2 n_{\mathrm{e}}} \frac{\mathrm{Im}\,\epsilon^{-1}(\mathrm{k},\omega)}{1 - \exp\left(-\frac{\hbar\omega}{k_{\mathrm{B}} T_{\mathrm{e}}}\right)}.$$

B. Witte et al., PRL **118**, 225001 (2017)

XRTS in isochorically heated Al

$$\alpha(\omega) = \frac{4\pi\sqrt{2}}{\sqrt{|\epsilon(\omega)|^2 + \mathrm{Re}[\epsilon(\omega)]}} \mathrm{Re}[\sigma(\omega)]$$

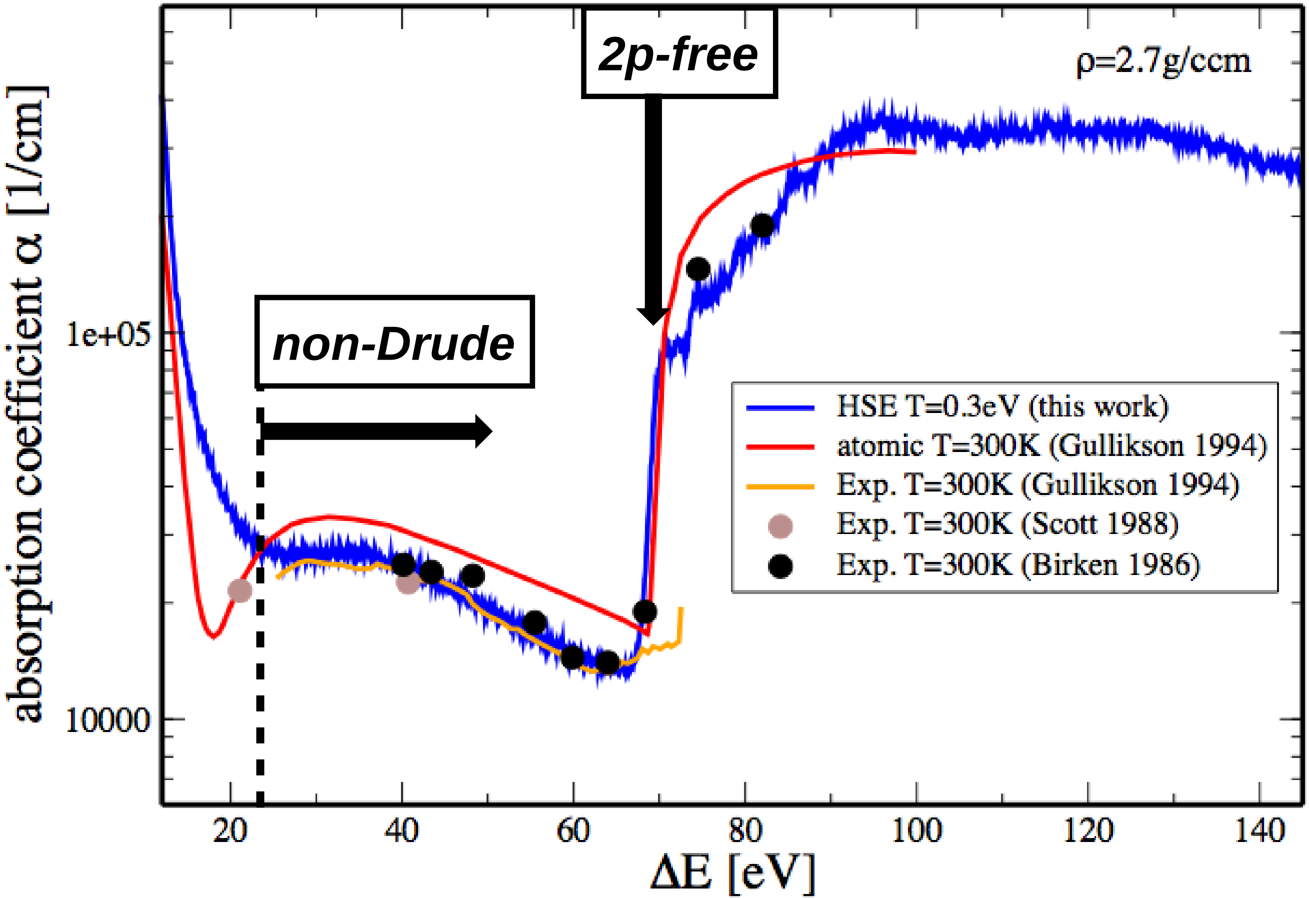

B. Witte et al., PRL **118**, 225001 (2017)

XRTS in isochorically heated Al

$$S_{et}(k \to 0, \omega) = -\lim_{k \to 0} \frac{\epsilon_0 \hbar k^2}{\pi e^2 n_e} \frac{\mathrm{Im}\left[\epsilon^{-1}(k,\omega)\right]}{1 - \exp\left[\frac{-\hbar\omega}{k_B T_e}\right]}$$

Mermin approach for k-dependent plasmon

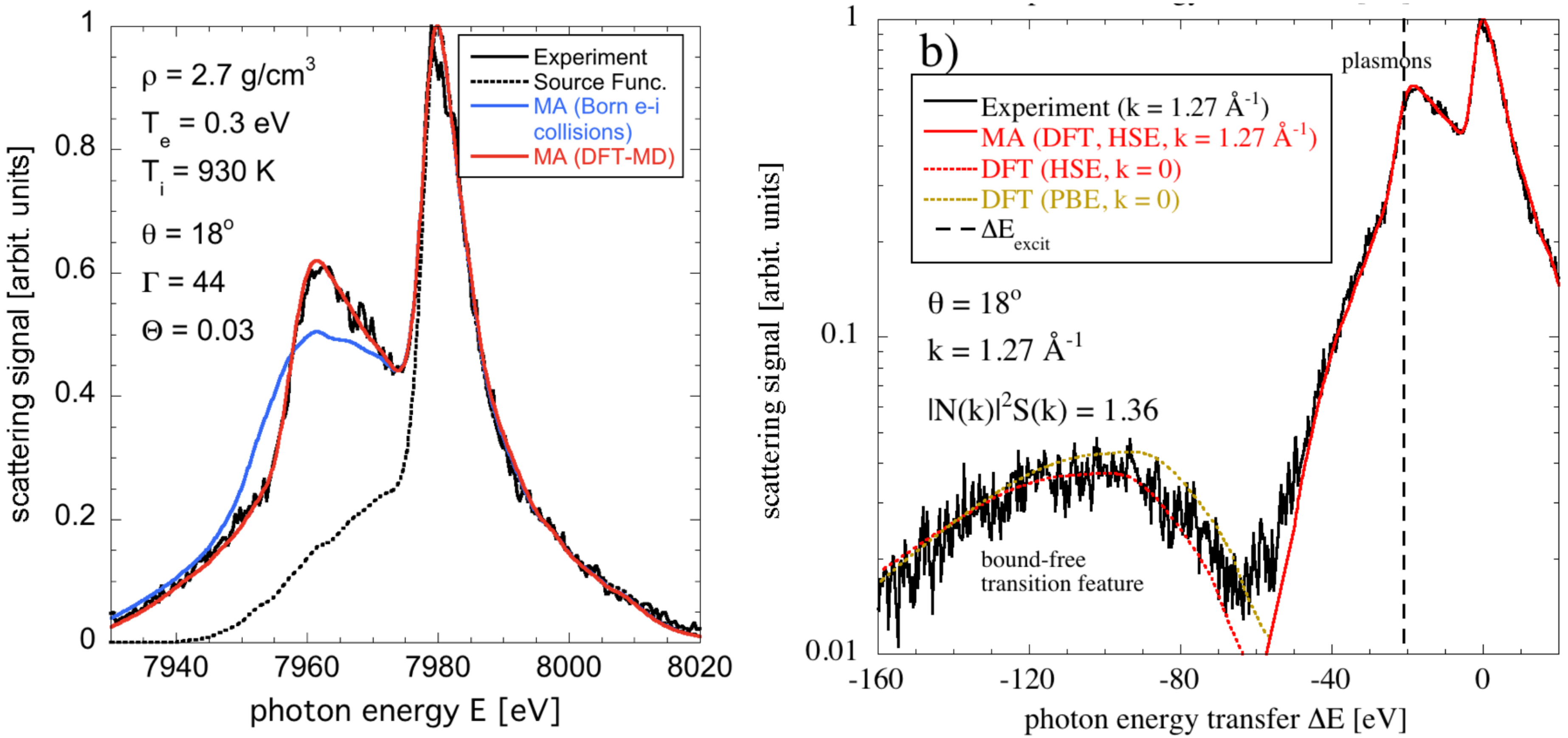

B. Witte et al., PRL **118**, 225001 (2017)

XRTS in isochorically heated Al

Plasmon width and dispersion

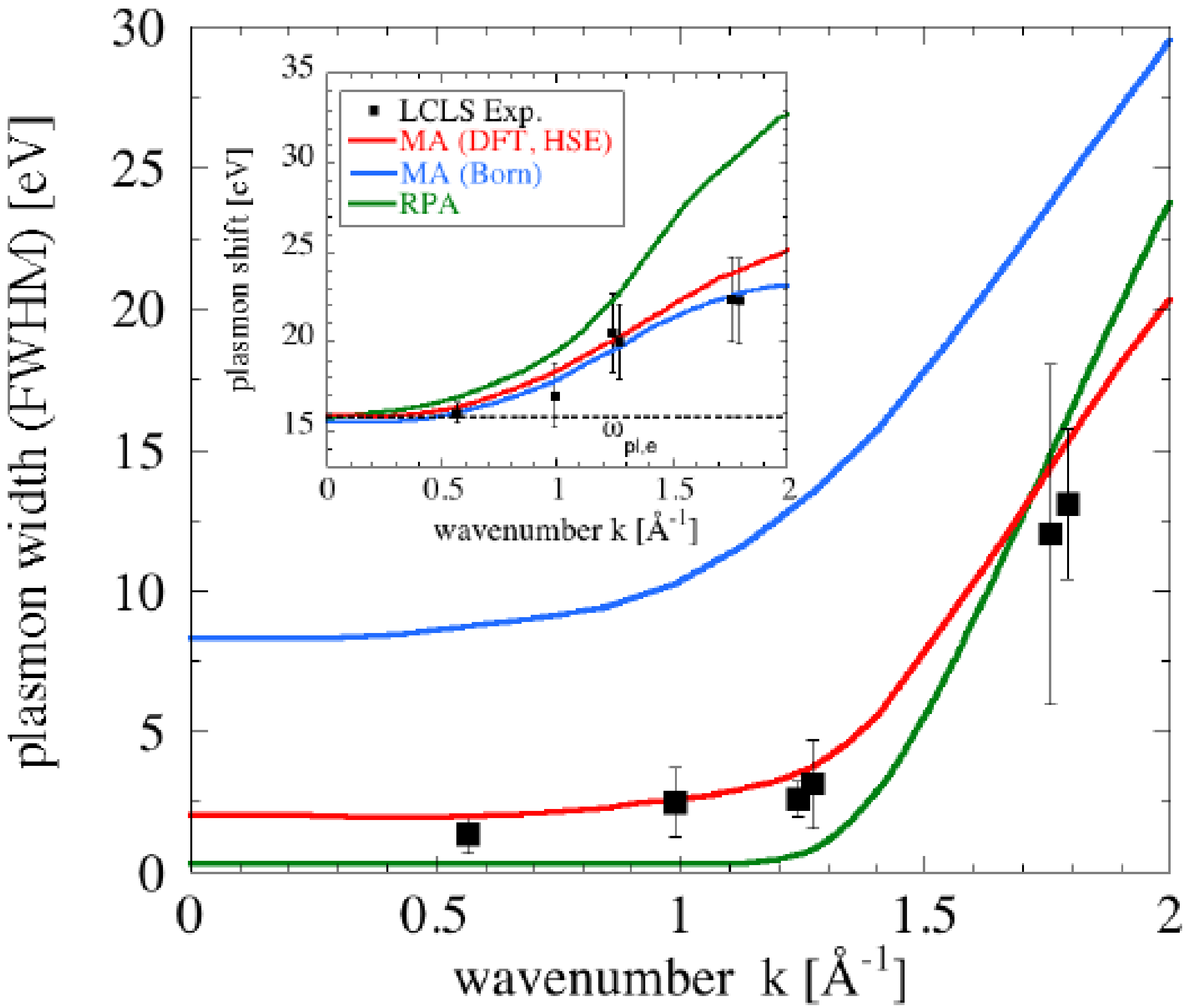

B. Witte et al., PRL **118**, 225001 (2017)

XRTS in isochorically heated Al

Electrical dc conductivity

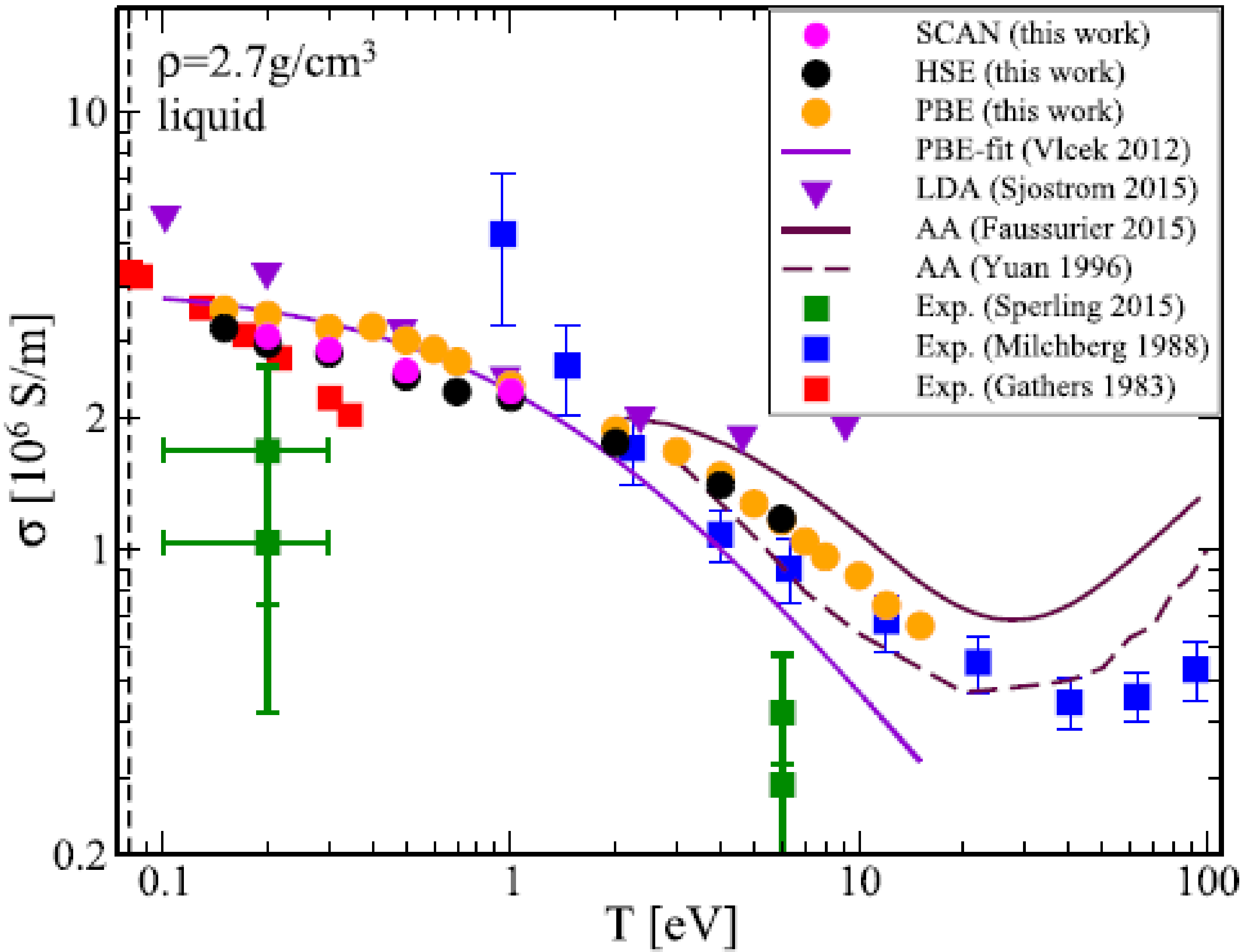

B. Witte et al., Phys. Plasmas **25**, 056901 (2018)

Contents

High-resolution inelastic X-ray scattering
Implementation at HED@XFEL

- Monochromator with different bandwidths:
  - $\Delta E/E = 10^{-3}$: SASE
  - $\Delta E/E = 10^{-4}$: Si_{111} monochromator
  - $\Delta E/E = 10^{-5}$: seeded
  - $\Delta E/E = 10^{-6}$: Si_{533} at 7.5 keV

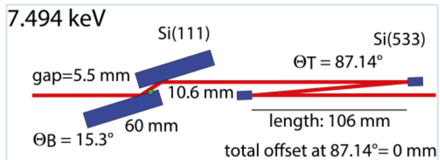

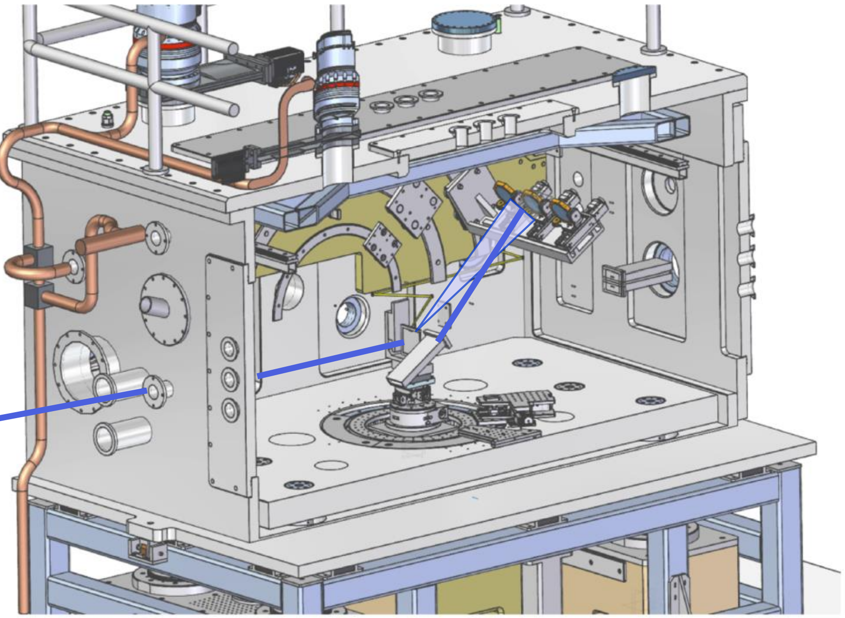

- 4 diced analyzer crystals from Si533 (ΔE=25 meV)
  - 3 in forward direction, →collective modes
  - 1 in backward scattering
    →Doppler broadening → ion temperature T_i

- **Dynamic ion structure factor** allows accessing
  - dissipative processes
  - viscosity
  - thermal conductivity
  - diffusive modes at Δk=0

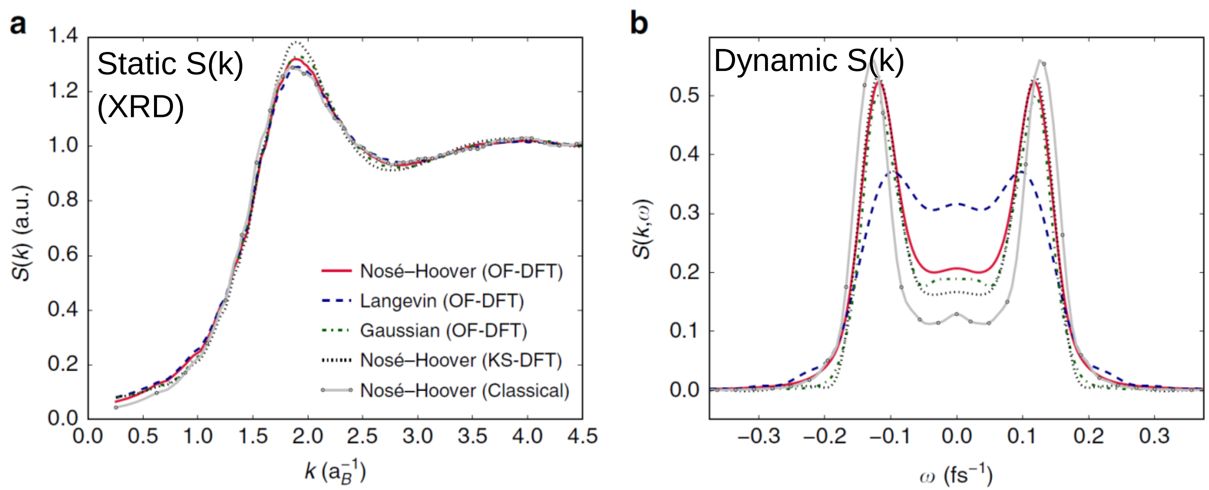

for warm dense aluminum: P. Mabey et al., Nat. Comm. 14125 (2017)

European XFEL

By courtesy of U. Zastrau

Ion dynamics - hydrodynamic model

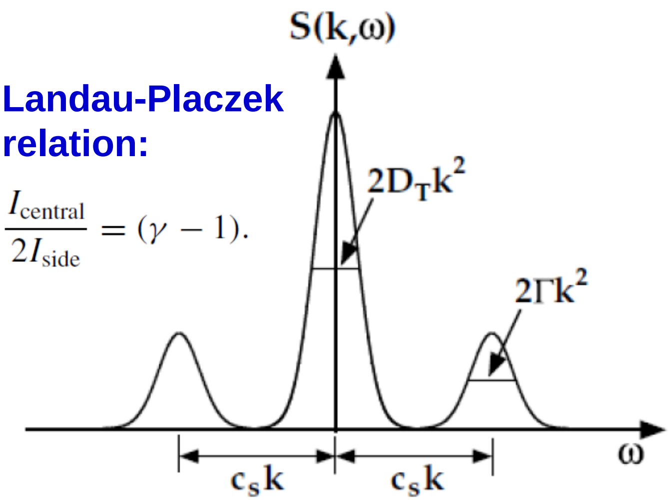

Landau-Placzek relation:

$$\frac{I_{\text{central}}}{2I_{\text{side}}} = (\gamma - 1).$$

$$2\pi \frac{S_{ii}(k,\omega)}{S_{ii}(k)} = \left(\frac{\gamma-1}{\gamma}\right) \frac{2D_T k^2}{\omega^2 + (D_T k^2)^2} + \frac{1}{\gamma}\left(\frac{\Gamma k^2}{(\omega + c_s k)^2 + (\Gamma k^2)^2} + \frac{\Gamma k^2}{(\omega - c_s k)^2 + (\Gamma k^2)^2}\right)$$

- Liquid: Rayleigh line centered at $\omega = 0 \rightsquigarrow$ diffusive thermal mode
- Width given by thermal diffusivity $D_T = \frac{a}{\gamma} = \frac{\lambda}{\varrho c_p}$ with $\gamma = \frac{c_p}{c_v}$ and $a = \frac{\lambda}{\varrho c_v}$
- Two Brillouin lines centered at $\omega = \pm c_s k$: ion acoustic modes with speed of sound c_s
- Width given by sound attenuation coefficient $\Gamma = \frac{a(\gamma-1)}{2\gamma} + \frac{b}{2}$
- Kinematic longitudinal viscosity $b = (\frac{4}{3}\eta + \zeta)/(\varrho m)$ with η shear and ζ bulk viscosity
- Intensity ratio of Rayleigh versus Brillouin peaks: $(\gamma - 1)\Gamma/D_T$

See J.-P. Hansen, I.R. McDonald, *Theory of Simple Liquids* (Academic Press, London, 1986)

$S_{ii}(k,\omega)$ for warm dense Al

T=3.5 eV, ρ=5.2 g/cm³
typical for recent XRTS experiments (spectrum), see Ma et al. (2013), Fletcher et al. (2015)

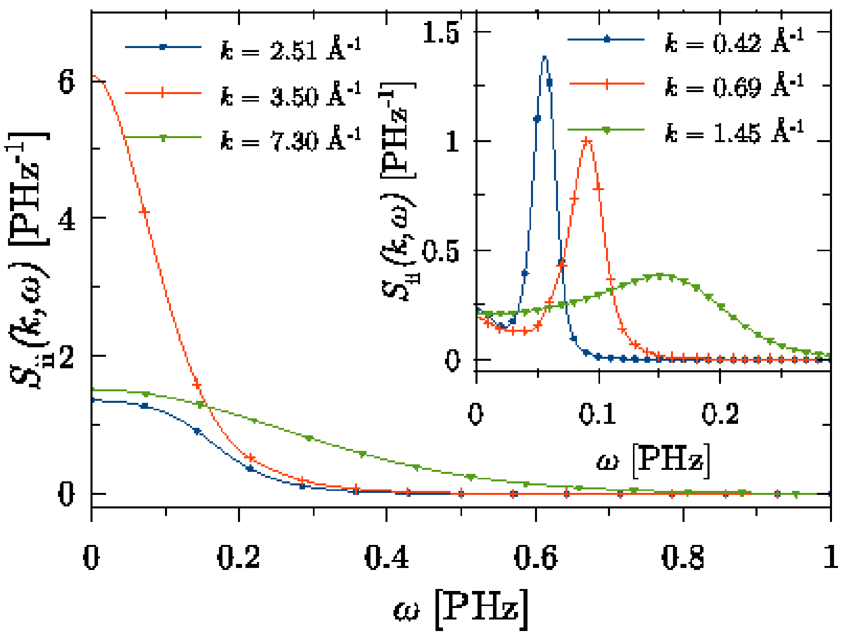

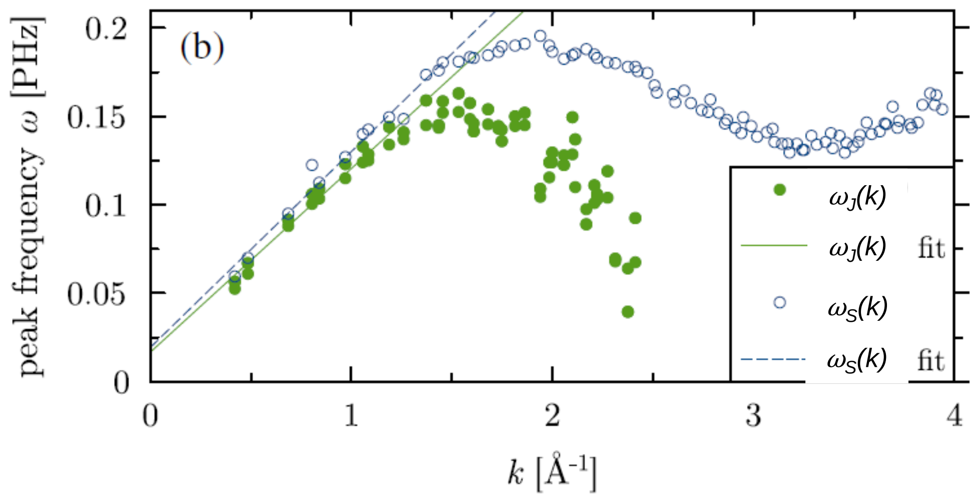

Ion acoustic modes: ω_s
Long. current correlation function: ω_l

TABLE I. Adiabatic and apparent sound velocity for liquid (1000 K, 2.3565 g/cm^3) and warm dense aluminum (40 600 K, 5.2 g/cm^3).

T (K)	ϱ (g/cm^3)	c_s (m/s)	c_l (m/s)
1000	2.3565	4860	5010
40 600	5.2	10 380	11 070

H.R. Rüter, RR, PRL **112**, 145007 (2014)
Based on full Kohn-Sham DFT-MD

Ion dynamics - generalized hydrodynamic model (GHM)

$$S_{\mathrm{ii}}^{\mathrm{GHD}}(\vec{k},\omega) = \frac{1}{2\pi}\left(\frac{2A\alpha}{\alpha^2+\omega^2} + \frac{B\beta}{\beta^2+(\omega_0+\omega)^2} + \frac{B\beta}{\beta^2+(\omega_0-\omega)^2} + \frac{C(\omega_0+\omega)}{\beta^2+(\omega_0+\omega)^2} + \frac{C(\omega_0-\omega)}{\beta^2+(\omega_0-\omega)^2}\right)$$

A, B, C (mode contributions: A diffusive, B: collective, C: shape), **α, β** (decay coefficients), $\boldsymbol{\omega_0}$ (position of side peaks) depend on k. A, B, C determined via the 0th, 1st and 2nd frequency moments, α, β, ω_0 are subject of a fitting procedure, see:

T. Bryk, J.F. Wax, J. Chem. Phys. **135**, 154510 (2011),
J.F. Wax, T. Bryk, J. Phys.: CM **25**, 325104 (2013).

Al: 10 eV, 8.1 g/cm³

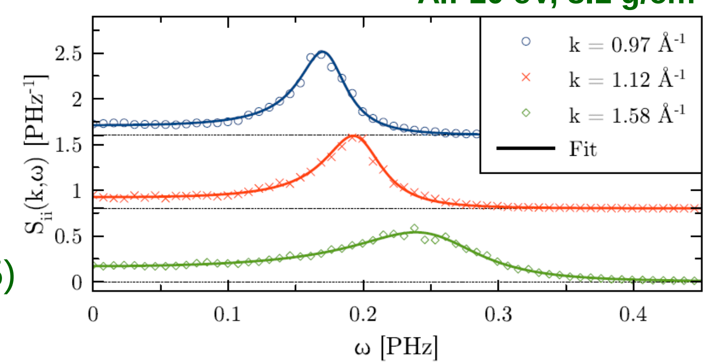

H.R. Rüter (2015)

Jupiter`s Interior with LM-REOS (H-He-H_2O)

Assuming a three-layer structure

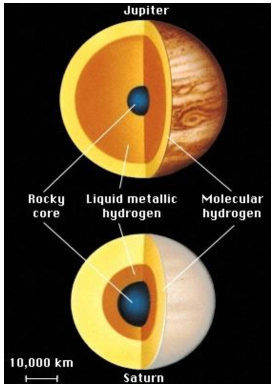

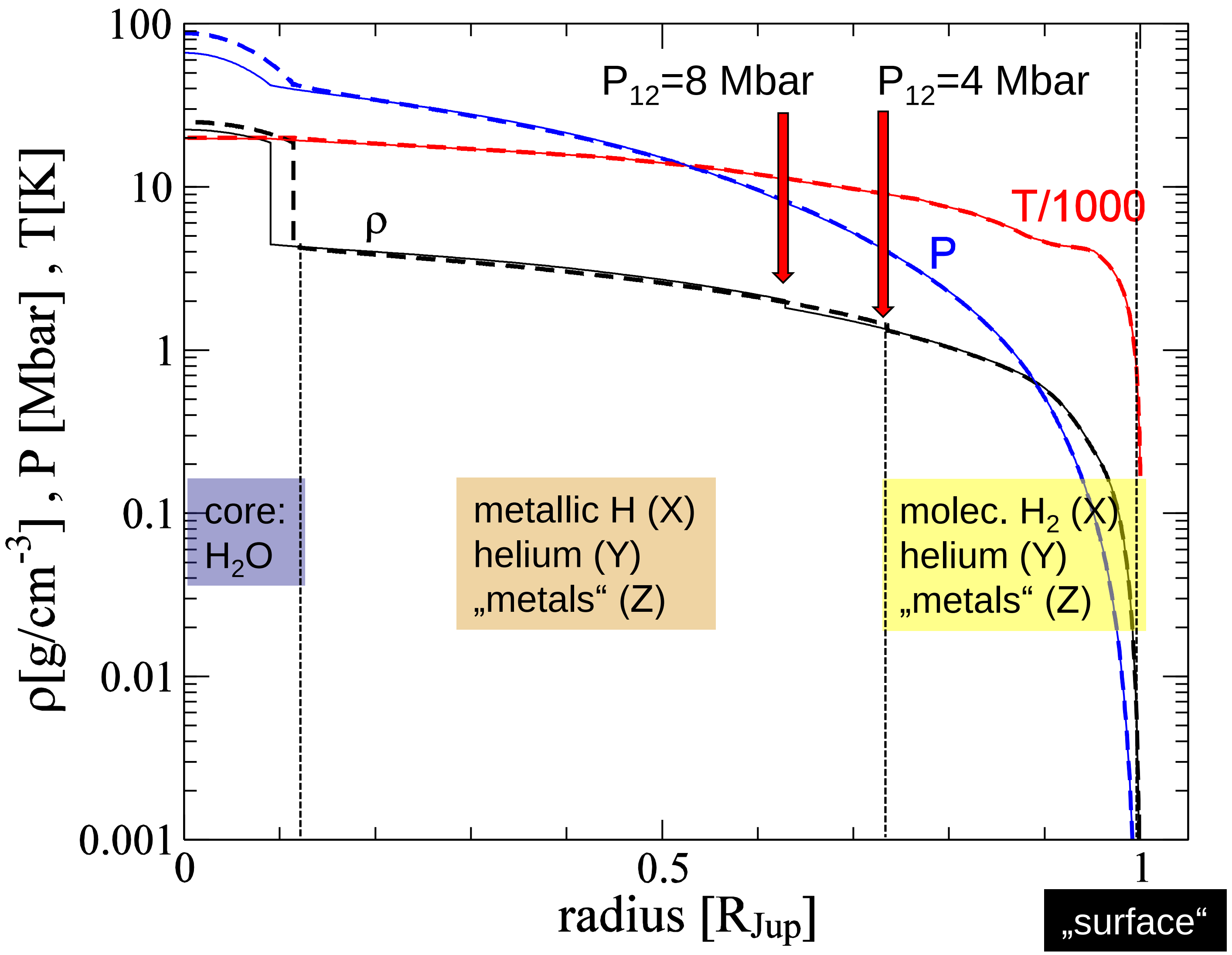

N. Nettelmann et al., ApJ **750**, 52 (2012), M. French et al., ApJS **202**, 5 (2012)

Material Properties along Jupiter`s Isentrope

M. French et al., ApJS **202**, 5 (2012): self-consistent EOS and material data from DFT-MD.
Used for planetary modeling (interior, dynamo, evolution)

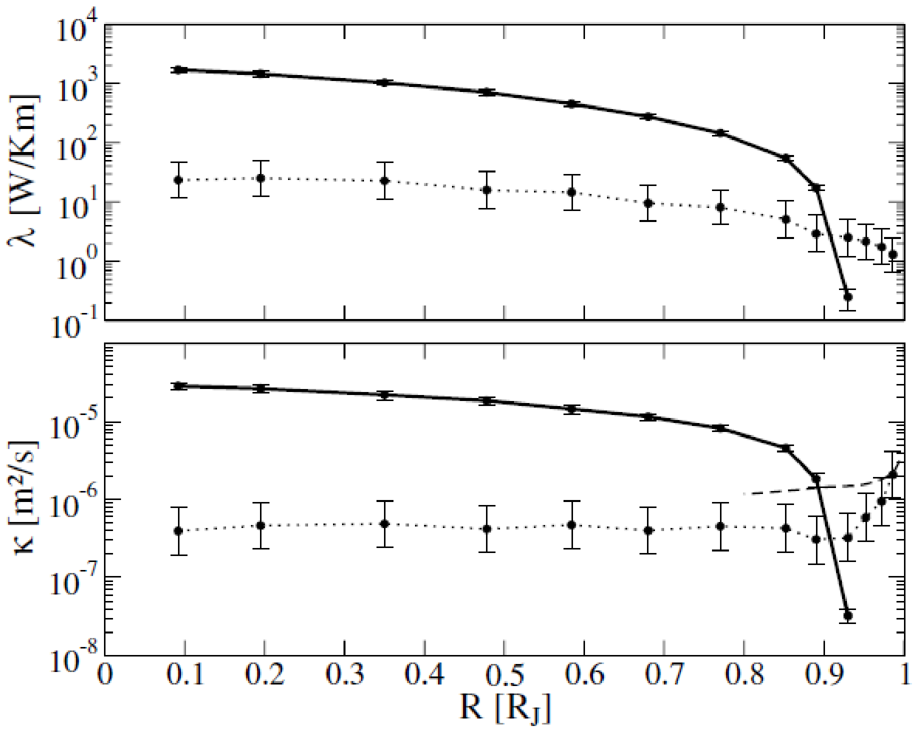

$\kappa = \lambda / (\rho c_p)$

Thermal conductivity λ and thermal diffusivity κ along Jupiter`s isentrope.

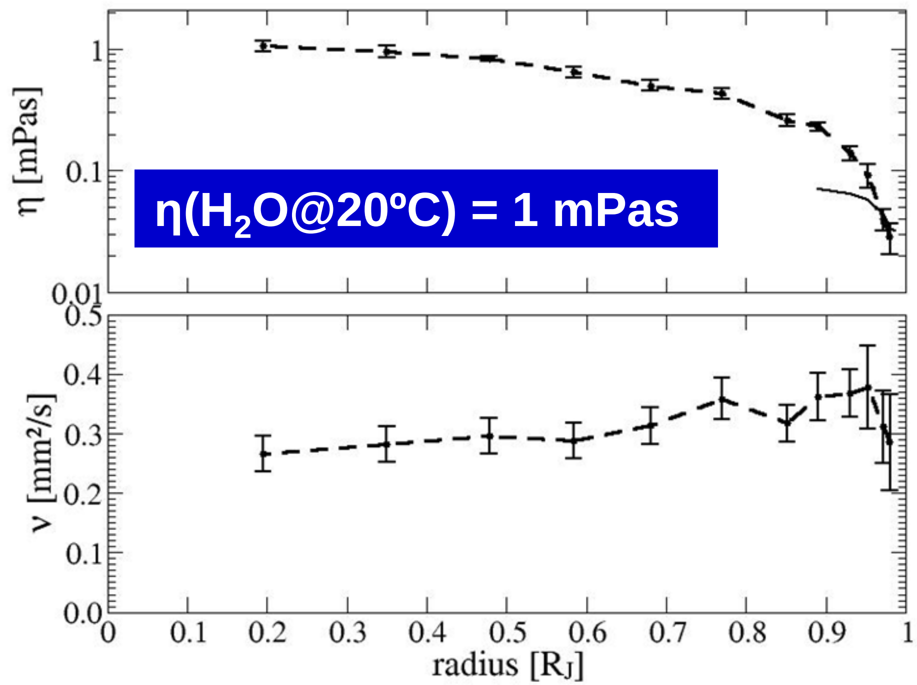

Dynamic (η) and kinematic (ν=η/ρ) viscosity along Jupiter`s isentrope.

$$\eta = \frac{\Omega}{3k_B T} \int_0^\infty dt \sum_{ij=\{xy,yz,zx\}} \left\langle p_{ij}(0)\, p_{ij}(t) \right\rangle$$

Summary & Outlook

- **Fundamental properties of WDM**

  → ab initio simulations are an essential tool for

  - **EOS data and high-pressure phase diagram**
  - **Dynamic structure factor: conductivities, viscosity**
  - **Relaxation times**

- **Plasma diagnostics: light-matter interaction**

  → rad-hydro and hydro simulations

  → analyze DAC and shock wave experiments

  → analyze XRTS experiments at FELs: DSF, DF

- **Application: planetary physics - understand**

  → diversity of solar/extrasolar planets

  → interior, evolution, magnetic field (dynamo)

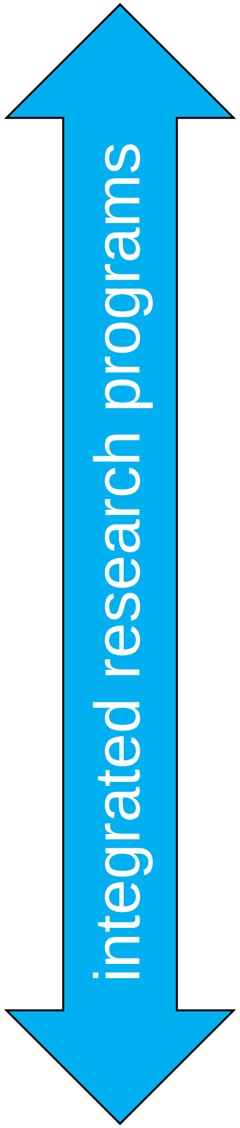

Upcoming Workshops & Conferences

16th Int. Conference on the Physics of Nonideal Plasmas (PNP-16)
September 24-28, 2018, Saint Malo

7th Joint Workshop on High Pressure, Planetary, and Plasma Physics (7HP4)
October 10-12, 2018, DLR Berlin

18th Int. Workshop on Radiative Properties of Hot Dende Matter (RPHDM 2018)
October 21-26, 2018, DESY Hamburg

12th Int. Workshop on Planetary Formation and Evolution (PFE-12)
Feb 27 – March 1, 2019, U Rostock

FOR 2440 „Matter Under Planetary Interior Conditions“

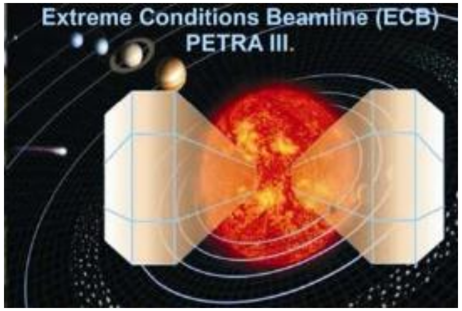

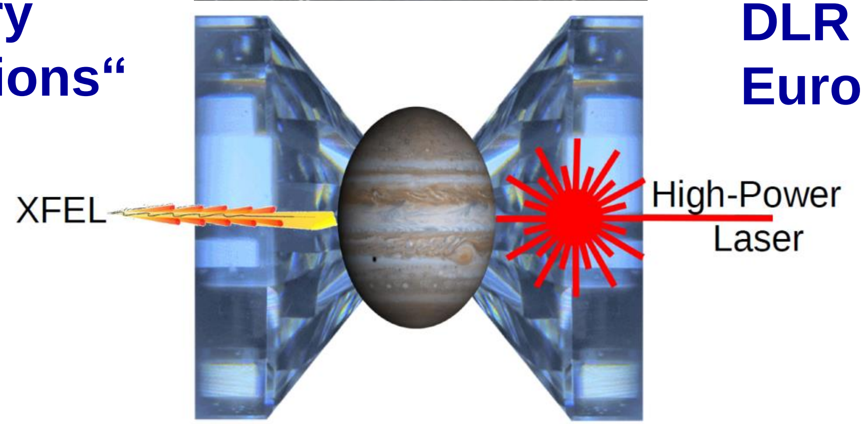

U Rostock
BGI Bayreuth
DESY
DLR Berlin
European XFEL